Dynamics of the glutathione/glutaredoxin system

Lefentse Nelly Mashamaite

BSc. (*Hons*) Genetics

Submitted in fulfilment of the academic requirements for the degree of

Master of Science

School of Life Sciences

University of KwaZulu-Natal

Pietermaritzburg

As the candidate's supervisor I have approved this dissertation for submission.

Name: Dr C.S. Pillay Signed: _____

Name: Prof. J.M. Rohwer Signed: _____

Preface

The experimental work described in this dissertation was carried out in the Discipline of Genetics, School of Life Sciences, University of KwaZulu-Natal, Pietermaritzburg, from March 2012 to December 2014 under the supervision of Dr C.S. Pillay and Prof. J.M. Rohwer.

These studies represent original work by the author and have not otherwise been submitted in any form to another University. Where use has been made of the work by other authors it has been duly acknowledged in the text.

Signed:

_____

Lefentse N. Mashamaite

February 2015

College of Agriculture, Engineering and Science
Declaration of Plagiarism

I, Lefentse Nelly Mashamaite declare that:

1. The research reported in this thesis, except where otherwise indicated is my original research.

2. This thesis has not been submitted for any degree or examination at any other university.

3. This thesis does not contain other persons' data, pictures, graphs or other information, unless specifically acknowledged as being sourced from other persons.

4. This thesis does not contain other persons' writing, unless specifically acknowledged as being sourced from other researchers. Where other written sources have been quoted, then:

    a. Their words have been re-written but the general information attributed to them has been referenced.

    b. Where their exact words have been used, then their writing has been placed in italics and inside quotation marks, and referenced.

5. This thesis does not contain text, graphics or tables copied and pasted from the Internet, unless specifically acknowledged, and the source being detailed in the thesis and in the References sections.

Signed:

_____

February 2015

Declaration Plagiarism 22/05/08 FHDR Approved

List of publications

Publications:

Pillay, C.S., Hofmeyr, J.H., Mashamaite, L.N., Rohwer, J.M., 2013. From top-down to bottom-up: computational modeling approaches for cellular redoxin networks. Antioxidants & redox signaling 18, 2075-2086

Mashamaite, L.N., Rohwer J.M., Pillay, C. S., 2015. The mono- and di- thiol mechanisms for glutaredoxin-dependent deglutathionylation are functionally equivalent: implications for redox systems biology. Bioscience Reports 35, e00173

ABSTRACT

The glutathione/glutaredoxin system is made up of glutaredoxins, glutathione (GSH) and glutathione reductase (GLR). Glutaredoxins, which are involved in essential cellular functions such as DNA synthesis, iron metabolism and iron-sulfur cluster assembly, become oxidised during their catalytic cycle and are reduced by GSH and GLR. Glutaredoxins also play a critical role in regulating the glutathionylation/deglutathionylation cycle. Under oxidative stress conditions, protein thiols may be glutathionylated and glutaredoxin activity is important for restoring the functions of these proteins. While the individual components of this system have been studied extensively, the dynamics of the system as a whole has not been described despite its importance in the glutathionylation/deglutathionylation process. Computational systems biology approaches could be used to describe this type of regulation but the kinetic mechanism used by glutaredoxins for deglutathionylation is unclear as a monothiol and a dithiol mechanism have both been proposed for glutaredoxin activity. The *in vitro* data supporting these mechanisms have been contradictory with a number of discrepancies observed in the literature, including contrasting activities of mutant glutaredoxin Cxx(C→S) and wild-type glutaredoxins. Further, Lineweaver-Burk plots showed a curved line pattern in some studies, while other studies reported a linear pattern in response to GSH. Finally, analyses of the Lineweaver-Burk plots in two substrate kinetics experiments revealed both parallel line and intersecting initial velocity line patterns for deglutathionylation. Computational and mathematical models were used to resolve these discrepancies and we showed that the mono- and di- thiol mechanisms, are in fact identical. Mathematical models of mutant and wild-type glutaredoxin activities revealed that the GSH concentration and the rate constant for GSH oxidation significantly affected these relative activities which explained the contradictory data for wild-type and mutant glutaredoxins. The sigmoidal response to GSH was due to the kinetic order of this reaction and our results demonstrated that the resulting parallel and intersecting kinetic line patterns observed in some studies depended on the reversibility of the deglutathionylation reaction. Finally, fitting experiments showed that our models were able to accurately describe the *in vitro* data. Collectively, our results showed how deglutathionylation should be described in computational systems biology models and further revealed how the formation of oxidised glutaredoxin may play a vital role in the regulation of glutaredoxin activity.

ACKNOWLEDGEMENTS

I would like to first and foremost thank my awesome supervisor Dr. Ché Pillay. No amount of words can express how grateful I am for all the assistance and guidance you have provided throughout my postgraduate years. I am truly thankful for the great opportunities; going to Cape Town was a fantastic experience. You have been a great mentor and I have learnt so much from you. It has truly been an honour working in your lab.

Thank you to Prof. Johann Rohwer for the all the positive input and the time and energy put into my project. It was a pleasure being supervised by someone with such brilliant insight.

I would like to thank the National Research Foundation for the generous scholarship I was awarded to pursue my MSc.

To Mommy and Daddy, I could write volumes about how much I appreciate all the love and support you've given me and that would still not be enough. Thank you for always inspiring me to be and to do better. I know I make you proud….KE A LE RATA, KE A LE LEBOGA.

My amazing sisters Lethabo, Lehlogonolo le Lebogang… Thank you for the love and encouragement, and most importantly the insane calls that actually kept me sane. I truly appreciate the constant laughs and crazy family moments. LOVE you ladies to infinity and beyond.

To my favourite nieces and nephew, Thato, Tshegofatso le Thakgatso. Thank you for bringing so much cheerfulness into my life. For all the Hugs and butterfly kisses…Mmane Fenyi adores you always.

My lab sisters, Tershy, MP, Bea and our adopted sisters Mary and Milly… Thank you for making B23 a wonderful place. Stay the beautiful people that you are!!!

My friends, Siphamandla Madikizela, Thulani Mashiane, Simphiwe Ngcobo, Ayanda Mthalane, Selaelo Rasefate, Nhlakanipho Ngubane and Ndumiso Nhlabathi, for all the different roles y'all played in my life. I'm grateful for each and every one of you for all your encouraging words and support and I'm glad to have met such wonderful people. I got mad love for you all… Thank you!!!

My friends and colleagues from DSRA, Samukelisiwe Dube, Lulu Mmakola, Philisiwe Makhaye, Thabani Chagi and Zama Zindela. "We dance all night"… It's been epic working with you all. Thank you for the awesome juice and games nights, on and off duty. 30 seconds with you was always too much fun.

LIST OF ABBREVIATIONS

ArsC	Arsenate reductase
BSA-SSG	Glutathionylated Bovine Serum Albumin
CSSG	Glutathionylated Cysteine
dNTPs	deoxyribonucleotides
GAPDH	Glyceraldehyde 3-phosphate dehydrogenase
GLR	Glutathione Reductase
Grx	Glutaredoxin
GrxSS	Intramolecular disulfide glutaredoxin
GrxSSG	Glutaredoxin mixed disulfide
$Grx(SH)_2$	Reduced glutaredoxin
GSH	Glutathione (Reduced)
GSSG	Glutathione (Oxidised)
HEDS	β-hydroxyethyl disulfide
k_{cat}	Catalytic constant
K_m	Michaelis constant
ODE	Ordinary Differential Equation
PAPS	3'-phosphoadenosine 5'-phosphosulfate
Prx	Peroxiredoxin
PSH/RSH	Protein substrate
PSSG/RSSG	Glutathionylated protein
PySCeS	Python Simulator for Cellular Systems
r^2	Regression coefficient
RNR	Ribonucleotide Reductase
ROOH	Organic hydroperoxide
ROS	Reactive oxygen species
R-SOH	Sulfenic acid
$R\text{-}SO_2H$	Sulfinic acid
$R\text{-}SO_3H$	Sulfonic acid
SOD	Superoxide dismutase
Srx	Sulfiredoxins

Trx	Thioredoxin
TrxR	Thioredoxin Reductase
β-ME	β-Mercaptoethanol
β-ME-SG	Glutathionylated β-Mercaptoethanol

CONTENTS

LIST OF TABLES

LIST OF FIGURES

Chapter 1: Introduction

1.1 Oxidative stress and diseases

In aerobic organisms, oxygen is essential for survival as it is used for oxidative phosphorylation and is an important co-factor for several enzymatic reactions including the synthesis of the deoxyribonucleotides (Toledano *et al.*, 2007; Kalyanaraman, 2013). Unfortunately, normal cellular metabolism generates reactive oxygen species (ROS) which can damage cellular components (Fig. 1.1; Cooke *et al.*, 2003). ROS may occur in the form of either free radicals, such as the highly reactive hydroxyl radical ($OH^{\bullet}$) or they may be non-radicals such as hydrogen peroxide (H_2O_2) (Mates *et al.*, 2010, 2012; Melis *et al.*, 2013; Storr *et al.*, 2013). These ROS are the major causes of oxidative stress which usually occurs as a result of an imbalance between ROS production and the scavenging activity of the cellular antioxidant defence mechanisms (Fig.1.1; Melis *et al.*, 2013).

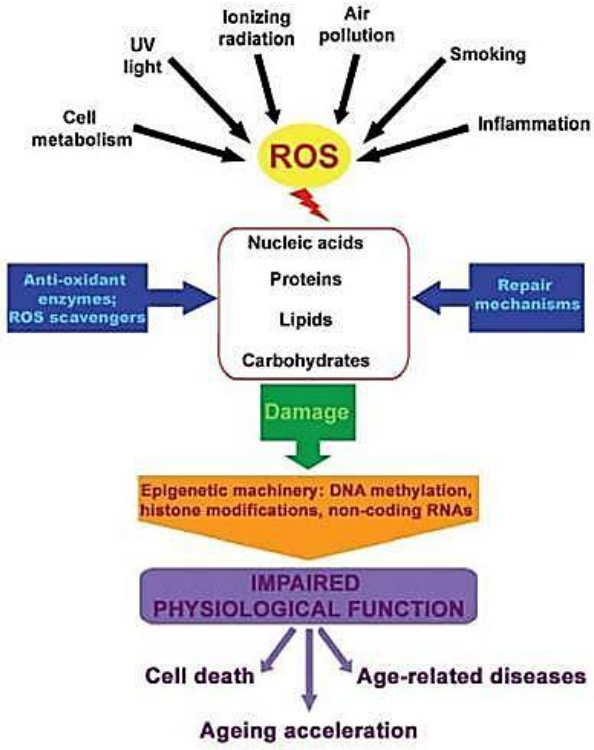

Figure 1.1. The action of oxidative stress on the cellular components leading to disease and cell death (Cencioni *et al.*, 2013). (Permission to reproduce this figure was granted by Multidisciplinary Digital Publishing Institute).

Oxidative stress poses an enormous risk to the survival of cells as it disrupts the redox homeostasis of the cell and may result in elevated levels of cellular damage, including oxidative DNA damage, alterations in the cytoplasmic and nuclear signalling as well as damage to lipids, carbohydrates and proteins (Fig. 1.1; Storr *et al.*, 2013). Protein cysteinyl residues specifically are sensitive to oxidative stress which may result in the formation of cysteinyl radicals, sulfenic, sulfinic or irreversible sulfonic acids. Alternatively, adjacent sulfhydryl groups within a protein or adjacent proteins may form disulfide bridges resulting in changes in protein conformation and/or aggregation (Dalle-Donne *et al.*, 2009). The extensive damage caused by oxidative stress on cellular molecules has been recognised as the cause of several diseases and may accelerate processes such as aging (Fig. 1.2; Melis *et al.*, 2013; Storr *et al.*, 2013).

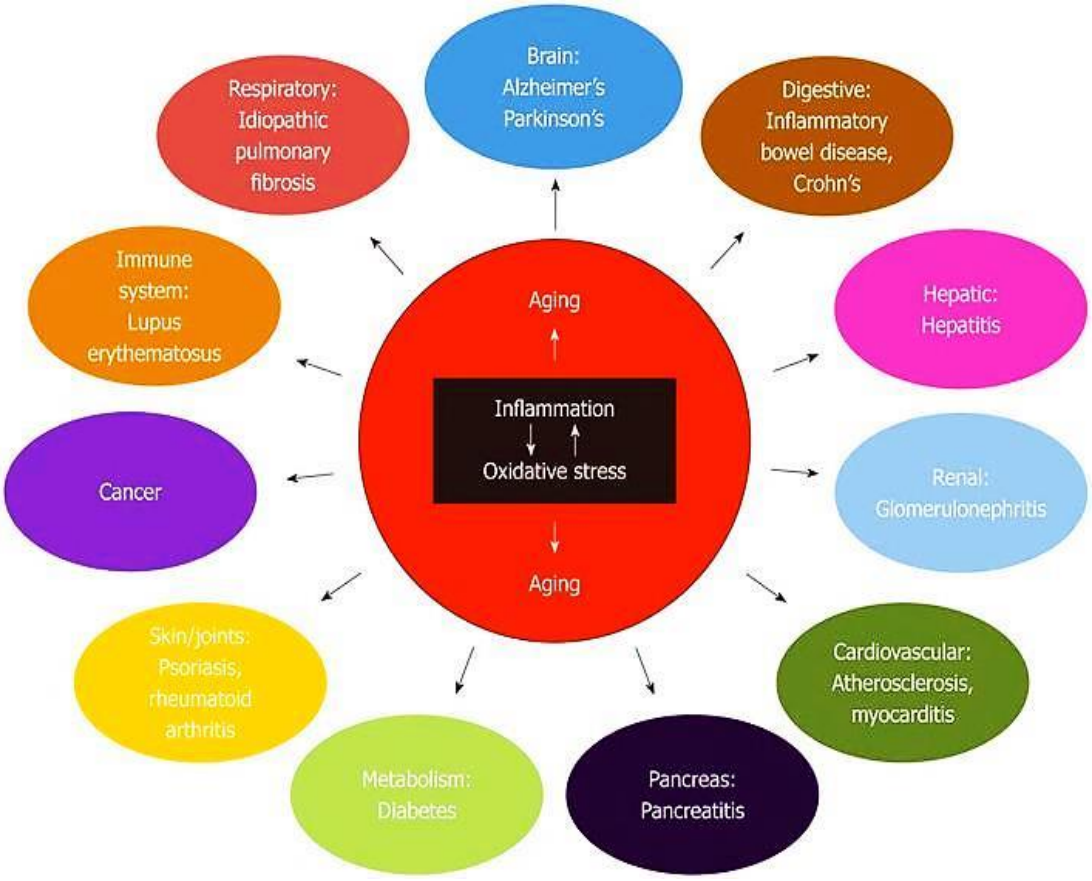

Figure 1.2. Diseases caused by the effect of oxidative stress (Terlecky *et al.*, 2012). (Permission to reproduce this figure was granted by Baishideng Publishing Group Inc.)

Several diseases have been linked to oxidative stress-induced DNA mutation (Fig. 1.2; Cooke *et al.*, 2003). DNA mutations induced by ROS may alter cellular signalling, leading to the inactivation of several tumour suppressor genes or alternatively, these

mutations may result in apoptosis which may be potentiated by ROS in many different cell types (Mates *et al.*, 2008; Raj *et al.*, 2011). Apoptosis is an important regulatory process in tumour expansion and the inhibition of apoptosis has been associated with many types of cancers (Kabore *et al.*, 2004; Miura *et al.*, 2011; Zhao *et al.*, 2012). Interestingly, many cancer tumours have shown elevated amounts of oxidative stress lesions and studies have shown that the elevated levels of damage were due to the low amounts of antioxidant enzymes in relation to the high levels of ROS generation in the tumour environment (Toyokuni *et al.*, 1995). Further, it has been shown that an increase in DNA damage together with the permanent activation of transcription factors and their associated genes resulting from elevated ROS creates a selection pressure for the malignant phenotype observed in cancer thus implicating oxidative DNA damage in the aetiology of cancer (Toyokuni *et al.*, 1995; Cooke *et al.*, 2003). Thus, ROS play important but contradictory roles in both apoptosis and cancer (Mates and Sanchez-Jimenez, 2000).

Oxidative stress has also been implicated in the pathogenesis of several neurodegenerative conditions (Fig. 1.2). Alzheimer's disease for example, is a condition characterised by progressive dementia and affects a vast number of the aging population (Cooke *et al.*, 2003). Oxidative stress in Alzheimer's disease may be caused by an imbalance between radical detoxifying enzymes and the free radicals that are formed during oxidative stress (Butterfield *et al.*, 2006; Gella and Durany, 2009). In affected patients, the brain tissue is exposed to elevated oxidative stress resulting in an excess of toxic ROS, numerous changes in cellular processes and the oxidation of DNA and RNA molecules (Fig. 1.1; Butterfield *et al.*, 2006). Further, the reduction in brain and plasma antioxidant defence mechanisms strongly correlates with memory loss due to age (Butterfield *et al.*, 2006; Gella and Durany, 2009).

Neurodegeneration as a result of oxidative stress has also been observed in patients with Parkinson's disease. The primary cause of Parkinson's disease is the advanced degeneration of neurons containing dopamine located in the zona-compacta of the substantia nigra (Alam *et al.*, 1997). The connection between Parkinson's disease and oxidative stress has been shown by various studies performed on post-mortem tissue where increases in iron levels (Sofic *et al.*, 1988; Dexter *et al.*, 1989; Riederer *et al.*, 1989) and superoxide dismutase (SOD) activity (Saggu *et al.*, 1989) were observed in the substantia nigra together with a

decrease in the levels of the thiol antioxidant GSH (Perry and Yong, 1986; Sofic *et al.*, 1992; Sian *et al.*, 1994).

Inflammatory conditions, infections such as hepatitis C, as well as atopic dermatitis are also associated with elevated levels of oxidative lesions. ROS, particularly the superoxide anion and hydrogen peroxide, are produced during the respiratory burst of neutrophils, macrophages and eosinophiles as bactericidal species. These species cause damage to the surrounding tissues generating oxidative stress conditions (Cooke *et al.*, 2003). These ROS are a major cause of connective tissue damage resulting in the formation of modified biomolecules which can trigger autoimmune diseases such as rheumatoid arthritis and systemic lupus arythematosus (Fig. 1.2) which consequently have oxidative stress implicated in their pathogenesis (Cooke *et al.*, 2003).

1.2 Cellular protective mechanisms

As oxidative stress is the basis for so many complications and diseases within cells, it is important that its effects are appropriately moderated. A number of proteins are responsible for regulating the levels of ROS within the cell as well as regulating redox-sensitive signalling pathways and maintaining a balance in the redox environment of the cell (Storr *et al.*, 2013). These mechanisms can be broadly divided into non-thiol and thiol mechanisms although these mechanisms are closely integrated *in vivo* to protect cells against oxidative stress (Mates *et al.*, 1999).

1.2.1 Non-thiol antioxidant enzymes

Superoxide dismutase (SOD) and catalase are the major non-thiol mechanisms used to counteract the effects of oxidative stress (Mates *et al.*, 1999). Superoxide dismutase specifically, is important as it catalytically enhances the normal dismutation of the superoxide anion to hydrogen peroxide and oxygen (Fig. 1.3; Kalyanaraman, 2013; Storr *et al.*, 2013). It increases the rate constant of normal dismutation from 10^5 M^{-1} s^{-1} to 10^9 M^{-1} s^{-1}, thus lowering the ambient superoxide concentration (Kalyanaraman, 2013). Superoxide dismutase produces hydrogen peroxide as a primary product in its catalytic cycle, which in turn is detoxified by catalases and peroxidases (Storr *et al.*, 2013).

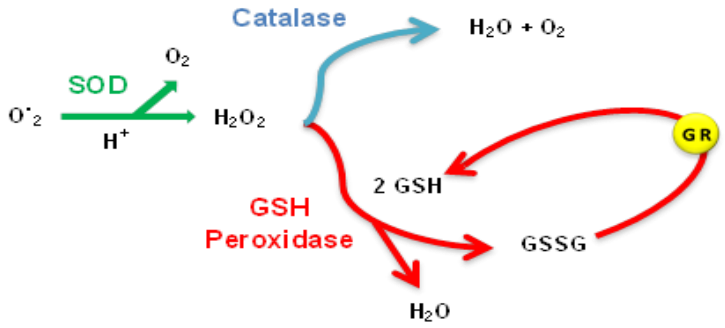

Figure 1.3. Activity of the three important cellular non-redoxin antioxidant defence enzymes, superoxide dismutase (SOD), catalase and glutathione (GSH) peroxidase.
(This figure was adapted from Proctor and Reynolds, 1984)

Catalase is an antioxidant enzyme, located in the peroxisomes of mammalian cells (Kalyanaraman, 2013) and converts hydrogen peroxide to water and oxygen (Fig. 1.3; Storr *et al.*, 2013). Catalase is especially important in cardiovascular disease as it has been shown that the overexpression of catalase together with superoxide dismutase impedes the progression of atherosclerosis, one of the main health problems leading to cardiovascular morbidity and mortality (Storr *et al.*, 2013).

1.2.2 Thiol antioxidant mechanisms

Thioredoxins, glutaredoxins and peroxiredoxins are the key components of the thiol redox systems that are involved in protecting the cells against ROS (Toledano *et al.*, 2007; Storr *et al.*, 2013). Thioredoxins and glutaredoxins are regarded as general disulfide reductases that also function in maintaining the thiol redox homeostasis of the cell (Trotter and Grant, 2003). Peroxiredoxins together with GSH peroxidases are ubiquitous non-heme peroxidases (Dayer *et al.*, 2008) that play an important role in removing ROS from cells thus protecting the cell against oxidative stress (Wood *et al.*, 2003). The activities of these redoxins will be discussed in greater detail below.

1.2.2.1 Peroxiredoxins

Peroxiredoxins were discovered initially in yeast as enzymes providing protection against damage caused by oxidative stress (Kim *et al.*, 1988). These redoxins were subsequently identified in many other biological kingdoms from bacteria to mammals and are

highly abundant in cells making up to 1% of the cellular protein content in some cells (Forman *et al.*, 2010; Rhee *et al.*, 2012). They are separated into three different classes, 1-Cys, typical 2-Cys and atypical 2-Cys depending on the number of cysteine residues directly involved in catalysis (Chae *et al.*, 1994; Wood *et al.*, 2003). Typical 2-Cys peroxiredoxins are obligate homodimers containing two identical active sites (Hirotsu *et al.*, 1999; Wood *et al.*, 2002) whereas the atypical 2-Cys peroxiredoxins are functionally monomeric (Seo *et al.*, 2000; Declercq *et al.*, 2001). These proteins are localised mainly in the cytosol but certain isoforms can also be found in the mitochondria and nuclei (Wood *et al.*, 2003).

Saccharomyces cerevisiae has five different peroxiredoxin isoforms (Rhee *et al.*, 2003) whereas mammalian cells have six different isoforms with each peroxiredoxin possessing a conserved cysteine residue in the N-terminal region of the active site region of each isoform (Storr *et al.*, 2013). Peroxiredoxins play a major role in the redox regulation of cell signalling and differentiation through the regulation of hydrogen peroxide levels within the cytosol (Rhee *et al.*, 2012). They also function in the reduction of alkylhydroperoxides and peroxynitrites (Dayer *et al.*, 2008). Furthermore, peroxiredoxins function as molecular chaperones and as phospholipase A2 enzymes (Chen *et al.*, 2000; Hanschmann *et al.*, 2013).

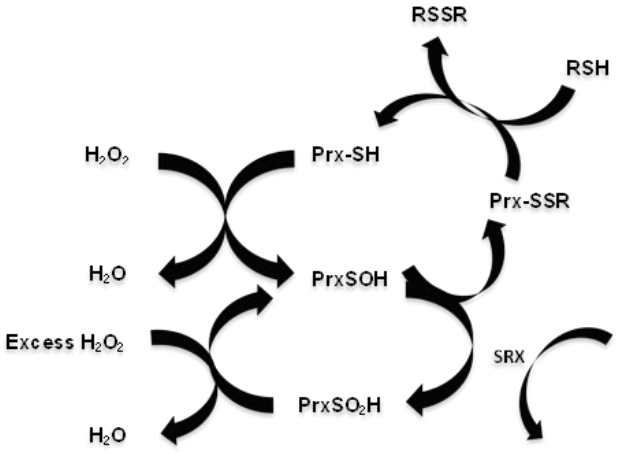

Figure 1.4. Reaction mechanism of the peroxiredoxins. This cycle applies to both, 1-Cys and 2-Cys peroxiredoxins (Prx) and further shows the reducing activity of sulfiredoxins (Srx). (This figure was adapted from Jacob *et al*., 2004)

Arguably the most significant function for peroxiredoxins is to reduce and detoxify hydrogen peroxide and organic hydroperoxides (ROOH) under oxidative stress conditions (Wood *et al.*, 2003; Du *et al.*, 2013). The N-terminal active site cysteine residue in peroxiredoxins (peroxidatic cysteine) reacts with either hydrogen peroxide or ROOH forming

a sulfenic acid intermediate in the partial reduction of these substrates to water or ROH respectively (Fig. 1.4; Hanschmann *et al.*, 2013). The cysteine-sulfenic acid intermediate reacts with the C-terminal cysteine residue (resolving cysteine) that occurs in another subunit in the case of the typical 2-Cys peroxiredoxins, resulting in an intermolecular disulfide or intramolecular disulfide bond in the case of the atypical 2-Cys peroxiredoxins. These bonds are reduced by thioredoxin in order to regain the active peroxiredoxin form (Wood *et al.*, 2003; Rhee *et al.*, 2005; Lu and Holmgren, 2014). In the presence of excess peroxide, peroxiredoxins may become over-oxidised resulting in the formation of sulfinic as well as sulfonic acids on the N-terminal active site cysteine. Sulfonic acids are considered to be irreversible protein modifications under physiological conditions, but sulfiredoxins (Srx) were identified as reductants of sulfinic acids *in vivo* (Fig. 1.4; Wood *et al.*, 2003; Findlay *et al.*, 2005).

1.2.2.2 Thioredoxins

Thioredoxins (Trx) were discovered in 1964 as essential cofactors for ribonucleotide reductase (RNR) (Laurent *et al.*, 1964). Thioredoxin and thioredoxin reductase (TrxR) make up the thioredoxin system, which is essential in the regulation of the intracellular redox state. Thioredoxin is present in numerous species and possesses a conserved active site that is characteristic of the thioredoxin superfamily (CxxC/S) (Holmgren, 2000).

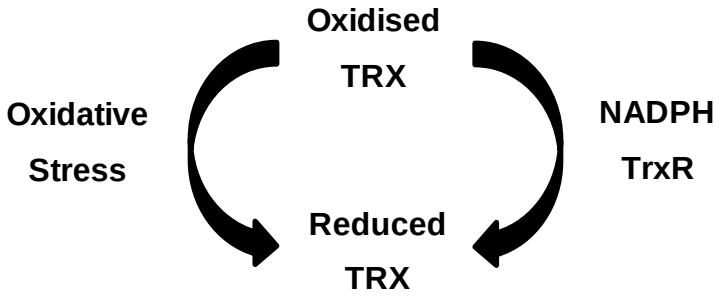

Figure 1.5. Scheme of the thioredoxin antioxidant system in the presence of oxidative stress. Oxidised thioredoxin (TRX) is reduced by thioredoxin reductase (TxrR) in the presence of NADPH and re-oxidised under oxidative stress conditions or during physiologically relevant reduction activities. (This figure was adapted from Akterin *et al*., 2006)

In the thioredoxin system, electrons are transferred from NADPH through the activity of thioredoxin reductase to the thioredoxin active site. Upon the reduction of a target protein,

this active site becomes oxidised (Fig. 1.5; Holmgren and Lu, 2010; Du *et al.*, 2013) and thioredoxin reductase then recycles the disulfide back into its dithiol form (Fig. 1.5; Holmgren, 2000). Thioredoxins play an important role in the defence against oxidative stress by providing the necessary electrons for the peroxiredoxins in the cell. Interestingly, human Trx1 possesses three non-active site cysteine residues (Cys62, Cys69 and Cys 73) in addition to their active site which have been implicated in the regulation of the activity of this thioredoxin (Du *et al.*, 2013). Under oxidising conditions, a second intramolecular disulfide distinct from the active site disulfide bond has been observed in these thioredoxins (Watson *et al.*, 2003; Du *et al.*, 2013) which disrupts the interaction that occurs between thioredoxin and its target proteins and inactivates Trx1 activity (Du *et al.*, 2013). These non-active site cysteines may also possess the ability to transfer electrons to peroxiredoxins (Du *et al.*, 2013). In summary, thioredoxins work together with the peroxiredoxins in antioxidant activity, where peroxiredoxins use electrons donated by the thioredoxin in scavenging intracellular ROS (Storr *et al.*, 2013).

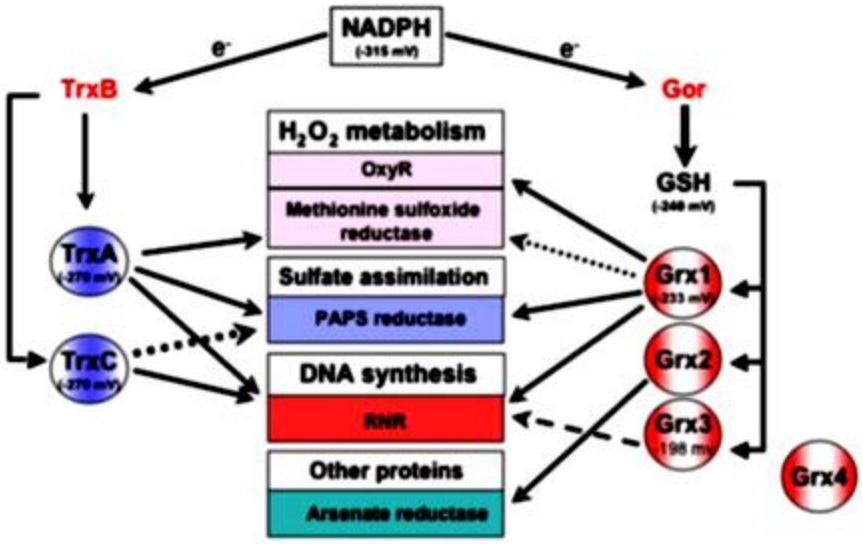

Figure 1.6. Components of the thioredoxin and glutaredoxin system in *Escherichia coli* with arrows showing the flow of electrons to the processes and targets of these redoxins (Toledano *et al*., 2007). (Permission to reproduce this figure was granted by Elsevier publishing company)

Thioredoxins as well as glutaredoxins (Grx) have been conserved throughout evolution and significant functional redundancy between these two systems has been recognised with regards to ribonucleotide reductase (RNR) which reduces ribonucleotides to deoxyribonucleotides (dNTPs), 3'-phosphoadenosine 5'-phosphosulfate (PAPS) reductase

(Fig. 1.6), and plasma GSH peroxidise activity (Lillig *et al.*, 1999). The thioredoxin system in *E. coli* consists of two thioredoxins which are encoded by *trxA* and t*rxC* and a thioredoxin reductase encoded by *trxB* (Fig 1.6; Miranda-Vizuete *et al.*, 1997). The GSH/glutaredoxin pathway consists of GSH, glutathione reductase encoded by *gor* and three glutaredoxins, Grx1, Grx2 and Grx3 which are encoded by *grxA*, *grxB* and *grxC* respectively (Fig 1.6; Holmgren, 1976; Aslund *et al.*, 1994). Normal aerobic growth is independent of either the thioredoxin or glutaredoxin branch individually, but when both systems are inactivated, cells are unviable as these systems are essential for ribonucleotide reductase activity (Fig. 1.6; Toledano *et al.*, 2007). Another function of these pathways in the *E. coli* system was shown when *trxA, gshA* and *grxA* or t*rxA* were mutated, resulting in the toxic accumulation of PAPS (Russel *et al.*, 1990). PAPS is an intermediate of sulfur assimilation and is reduced to sulfite by PAPS reductase which in turn is reduced by thioredoxin or glutaredoxin. Therefore, TrxA or Grx1 are necessary for sulfate assimilation and PAPS reductase reduction (Fig 1.6; Toledano *et al.*, 2007).

The cytosolic thioredoxin system in *S. cerevisiae* is made up of two thioredoxin genes, *TRX1* and *TRX2* and a thioredoxin reductase gene (Carmel-Harel and Storz, 2000). *S. cerevisiae* also has a GSH/glutaredoxin pathway performing similar functions to this thioredoxin pathway (Toledano *et al.*, 2007). While single and double yeast thioredoxin mutants are viable, the double mutant showed an extended S-phase due to inefficient ribonucleotide reductase reduction (Toledano *et al.*, 2007). This inefficiency has been established on the basis of a decrease in dNTP concentration as well as the reduced form of ribonucleotide reductase (Camier *et al.*, 2007). These results showed that although the GSH/glutaredoxin pathway was able to perform ribonucleotide reductase reduction in yeast, it was not as efficient as the thioredoxin pathway (Toledano *et al.*, 2007). Thioredoxins has been established as the sole hydrogen donor for PAPS reductase in *S. cerevisiae*, as the thioredoxin double mutant shows auxotrophy for sulfur amino acids (Draculic *et al.*, 2000).

Mammals have a large Trx-like protein (p23TrxL), a cytosolic Trx1 and a mitochondrial Trx2, all of which have a conserved active site (Storr *et al.*, 2013). The thioredoxin system is essential for survival in mammalian cells and also performs similar functions to the glutaredoxins, including the common role as hydrogen donors for ribonucleotide reductase in DNA synthesis (Martin, 1995). Both these systems also function in the regulation of apoptosis (Saitoh *et al.*, 1998; Chrestensen *et al.*, 2000), redox regulation

of transcription factors such as NFκB and AP-1 (Schenk *et al.*, 1994; Bandyopadhyay *et al.*, 1998; Hirota *et al.*, 2000) and in protein disulfide reduction (Holmgren, 1984; Stewart *et al.*, 1998).

1.2.2.3 Glutaredoxins

Glutaredoxins were identified as GSH-dependent reductases when growth of a thioredoxin mutant of *E. coli* was observed suggesting that another protein was able to reduce ribonucleotide reductase (Holmgren, 1979b). Glutaredoxins are evolutionarily conserved, heat-stable oxidoreductases with active sites which contain one or two cysteine residues (Holmgren and Aslund, 1995). Depending on the number of cysteine residues at the CxxC/S active site, glutaredoxins can be separated into monothiol or dithiol type glutaredoxins (Herrero and de la Torre-Ruiz, 2007; Eckers *et al.*, 2009). These glutaredoxins can further be grouped based on their physiological roles, subcellular localisation and biochemical properties (Eckers *et al.*, 2009). They are structurally all members of the thioredoxin superfamily as they have a thioredoxin fold but are distinguishable from thioredoxins by their specificity for GSH (Luikenhuis *et al.*, 1998; Eckers *et al.*, 2009).

As described above, while the GSH/glutaredoxin and thioredoxin systems are functionally redundant, *E. coli* double mutants lacking the components of both systems were not viable (Prinz *et al.*, 1997; Toledano *et al.*, 2007). Apart from the functions shared with the thioredoxin system (Fig. 1.6), glutaredoxins perform specialised functions within the cell, such as the reduction of arsenate reductase (ArsC) and the transcription factor OxyR (Fernandes and Holmgren, 2004). OxyR regulates the expression of Grx1, Trx2 and glutathione reductase (Gor; Fig. 1.6) and several other antioxidant defensive genes in response to increases in the hydrogen peroxide levels (Fernandes and Holmgren, 2004). In *E. coli* specifically, glutaredoxins also contribute to the defence against hydrogen peroxides with *gshA* and *grxB* mutants being more sensitive to hydrogen peroxide as shown by the elevation in carbonylation of intracellular proteins (Fernandes and Holmgren, 2004).

The GSH/glutaredoxin pathway in *S. cerevisiae* includes GSH, glutathione reductase (GLR) and two groups of glutaredoxins, the dithiol forms with a CxxC active site motif *(GRX1, GRX2* and the putative *GRX8)* and the monothiol forms with a CxxS active site motif (*GRX3, GRX4, GRX5, GRX6* and *GRX7)* (Toledano *et al.*, 2007; Li *et al.*, 2010). As with

E. coli, the viability of yeast cells is dependent on the presence of a single active glutaredoxin or thioredoxin system. The initial evidence of functional association between the thioredoxin and glutaredoxin systems in yeast arose from the recognition of a glutathione reductase non-viable mutant when screening for mutations presenting a need for thioredoxins (Muller, 1996).

Table 1.1. Phenotypes and characteristics of thiol redox system mutants in *Saccharomyces cerevisiae* (Toledano *et al*., 2007). (Permission to reproduce this table was granted by Elsevier publishing company)

Mutant	Phenotype	Rescued by	Defects
Δtrx1	nl[a]		
Δtrx2	nl		
Δtrr1	Slow growth		
Δtrx1Δtrx2	Protracted S phase, Met auxotrophy	RNR overexpression	Sulfate assimilation, Ribonucleotide reduction
Δtrr1Δtrx1Δtrx2	Similar to *Δtrx1Δtrx2*	Similar to *Δtrx1Δtrx2*	Similar to *Δtrx1Δtrx2*
Δglr1	nl		Accumulates GSSG
Δgrx1Δgrx2	nl		
Δgrx1Δgrx2Δtrx1Δtrx2	Unviable		Ribonucleotide reduction
Δtrx1Δtrx2Δglr1	Unviable aerobically	Anaerobic weak growth	Complex
Δtrr1Δglr1	Unviable aerobically		Complex
Δtrx1Δtrx2Δgsh1	Unviable aerobically	ND	Complex
Δgrx2Δgrx5	Unviable		Unknown
Δgsh1	GSH auxotrophy	0.5 μM GSH	Cytoplasmic [Fe–S] assembly
Δgrx1Δgrx2Δgrx3Δgrx4	nl		
Δgrx5	Slow growth	Grx3 and Grx4 targeted to mitochondria	Mitochondrial [Fe–S] assembly
Δgrx3Δgrx4Δgrx5	Unviable		[Fe–S] assembly
Δgrx3Δgrx4Δ	Slow growth		Cytoplasmic [Fe–S] assembly

[a]nl: Normal vegetative growth. All defect presented are hypothetical and have not been yet demonstrated experimentally. For references, see text.

Baker's yeast has provided an ideal eukaryotic organism for the analysis of the overlapping functions between the thioredoxin as well as the glutaredoxin systems (Draculic *et al.*, 2000). The triple *Δtrx1 Δtrx2 Δglr1* mutant (Table 1.1) had limited growth, which was repaired by employing anaerobic conditions showing that the viability of this particular strain was strongly related to oxidative stress. It was further shown that the lethality of this mutant did not occur due to problems in the synthesis of deoxyribonucleotides because adding reduced GSH did not restore viability in this mutant (Grant, 2001).

The functional overlap between the thioredoxin and the glutaredoxin systems was confirmed in other experiments. In the absence of both *TRX1* and *TRX2*, there was an elevation in the levels of GSSG which shows an association between the thioredoxin system and the GSH levels in the cell (Muller, 1996). The *Δtrx1* and *Δtrx2* mutant triggered changes in the GSH:GSSG ratio and caused an elevation in both the GSH and the GSSG concentrations while the *Δglr1* mutant resulted in an increase in the GSSG concentration.

Thus, the high intracellular GSH/GSSG ratio may be maintained by thioredoxins together with glutathione reductase (Trotter and Grant, 2003).

In mammalian cells glutaredoxins are involved not only in the reduction of ribonucleotide reductase but also in the reduction of dehydroascorbate (Wells *et al.*, 1990) and are especially important in maintaining the reduced state of the cellular protein cysteine residues (Gladyshev *et al.*, 2001). Glutaredoxins also play a key role in the glutathionylation/deglutathionylation cycle as described below.

1.3 Glutathionylation

The cysteinyl residues in proteins are particularly important in redox dependent modifications occurring during oxidative stress due to the sensitivity of the protein thiol group to oxidative alterations (Lillig *et al.*, 2008). Excess hydrogen peroxide can lead to the formation of sulfinic acid ($R\text{-}SO_2H$) or sulfonic acid ($R\text{-}SO_3H$) which cannot be reduced by cellular redoxin systems (Fig. 1.7; Lillig and Berndt, 2013). However, under less extreme oxidative stress conditions, protein thiol groups may undergo modifications resulting in the formation of sulfenic acid (R-SOH) and neighbouring protein thiols may form inter- or intra-molecular disulfide bonds between each other or with surrounding low molecular weight thiols such as GSH.

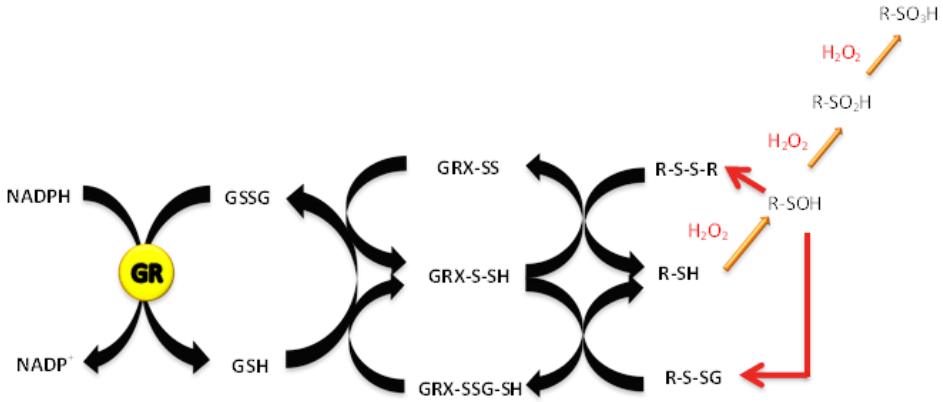

Figure 1.7. Reaction mechanism for the glutaredoxin system and the regulation of thiol modifications. (This figure was adapted from Lillig and Berndt, 2013)

The process whereby the GSH attaches to the thiol groups of protein cysteine is called glutathionylation and glutathionylated proteins (RSSG) may have altered activities and/or structures (Fig. 1.7; Lillig *et al.*, 2008; Dalle-Donne *et al.*, 2009). Glutathionylation is

particularly important as it not only protects the protein cysteine residues from irreversible oxidation, where protein structural and functional changes remain permanent, but it also functions in regulating the activity of the many target proteins (Rouhier *et al.*, 2004). The accumulation of glutathionylated proteins has been reported to occur under physiological and moderate oxidative stress conditions in various cell types, and GSH sometimes remains attached to the reactive cysteine residues of the intracellular proteins subsequent to the removal of the oxidative stress (Silva *et al.*, 2008). Under these moderate stress conditions glutathionylation plays an important role in redox regulation; furthermore, the glutathionylation of abundant proteins may serve as storage for GSH (Dalle-Donne *et al.*, 2009).

1.3.1 Target proteins of glutaredoxins

Glutathionylation has been observed in various organisms including plants, *E. coli*, yeast and in mammals. *In vivo* and *in vitro* proteomic labelling of sensitive targets with biotinylated GSSG were used to identify many protein targets for glutathionylation (Table 1.2; Rouhier *et al.*, 2004). In plants for instance, glutathionylation plays a role in various fundamental processes such as flowering (Ogawa *et al.*, 2001), root hair density and growth (Sanchez-Fernandez *et al.*, 1997; Lillig *et al.*, 2008). Plant proteins targets include aldolase (Ito *et al.*, 2003), triose phosphate isomerase (Ito *et al.*, 2003) and glutathione S-transferases (Dixon *et al.*, 2002) amongst others (Table 1.2). In some plants there is interaction between the thioredoxin and glutaredoxin systems with the poplar thioredoxin h isoform (Ptrc trxh4) (Table 1.2) being reduced by plant glutaredoxins (Gelhaye *et al.*, 2003) while the chloroplastic thioredoxin f (Table 1.2) is regulated by glutathionylation (Michelet *et al.*, 2005).

In *E. coli*, the transcription factor OxyR was identified as a target protein for glutaredoxin and is able to go through a number of stable processes such as nitrosylation, oxidation resulting in the formation of an intramolecular disulfide and glutathionylation (Lillig *et al.*, 2008) which result in post translational modifications of the regulatory thiol (SH). Changes in the structure, cooperative properties, DNA binding affinity as well as promoter activities of these altered forms of OxyR can be observed allowing for differentiated responses to redox signals (Zheng *et al.*, 1998).

Table 1.2. Examples of protein targets of glutaredoxin in various species (Rouhier *et al.*, 2004)

Plant targets	Aldolase (Ito *et al.*, 2003)
	Mitochondrial isoforms of thioredoxin h (Gelhaye *et al.*, 2003)
	Chloroplastic f-type Trxs (Michelet *et al.*, 2005)
	Chloroplastic glyceraladehyde 3-phosphatase dehydrogenase (Zaffagnini *et al.*, 2007)
	Protein tyrosin phosphatase (Dixon *et al.*, 2002)
Escherichia coli targets	OxyR (Zheng *et al.*, 1998)
	Ribonucleotide reductase (Holmgren, 1979b)
	PAPS reductase (Lillig *et al.*, 1999; Lillig *et al.*, 2003)
	Arsenate Reductase (Shi *et al.*, 1999)
Mammalian targets	PTP1B (protein tyrosine phosphatase 1B) (Barrett *et al.*, 1999)
	NF-*k*B (nuclear factor *k*B) (p50 subunit) (Hirota *et al.*, 2000; Klatt *et al.*, 2000)
	AP1 (activator protein 1) (c-jun subunit) (Bandyopadhyay *et al.*, 1998; Zheng *et al.*, 1998)
	Caspase-3 (Klatt *et al.*, 2000)
	HIV protease (Davis *et al.*, 1997)
	Actin (Wang *et al.*, 2001; Fratelli *et al.*, 2002; Lind *et al.*, 2002)
	Glyceraldehyde 3-phosphate dehydrogenase (Lind *et al.*, 2002)
	Creatine kinase (Klatt *et al.*, 2000)
	Enolase (Fratelli *et al.*, 2002; Lind *et al.*, 2002)
	Aldolase (Fratelli *et al.*, 2002)
Yeast targets	Alcohol dehydrogenase (Klatt *et al.*, 2000)
	Enolase (Shenton and Grant, 2003)
	GAPDH (Shenton and Grant, 2003)

Numerous mammalian protein targets (Table 1.2) undergo glutathionylation especially under oxidative stress conditions (Rouhier *et al.*, 2004). Interestingly, mammalian

glutaredoxins regulate peroxiredoxins and GSH peroxidase in response to oxidative stress and in so doing, regulate many transcription factors such as NF-*k*B, kinases and phosphatases in signalling pathways (Table 1.2; Rouhier *et al.*, 2004).

In yeast three protein targets for glutathionylation were recognised. With glyceraldehyde 3-phosphate dehydrogenase (GAPDH) in particular, two of the three described isoforms were irreversibly glutathionylated (Shenton and Grant, 2003). The third isoform of GAPDH, unlike the other two, is inhibited by glutathionylation but can be restored by deglutathionylation activity of the monothiol Grx5. Furthermore, yeast mutants lacking Grx5 show increased GAPDH glutathionylation and an inhibition of enzyme activity (Shenton *et al.*, 2002). In summary, a number of proteins involved in critical cellular processes may undergo glutathionylation (Table 1.2) emphasising how important the GSH/glutaredoxin system is within cells as a redox regulation mechanism (Dalle-Donne *et al.*, 2009).

1.3.2 Deglutathionylation of target proteins

Glutathionylation of protein targets can be reversed by deglutathionylation (Shelton *et al.*, 2005), where the GSH is removed from the thiol groups of protein cysteine residues, consequently regenerating the activities performed by these proteins (Fig. 1.8; Lillig *et al.*, 2008).

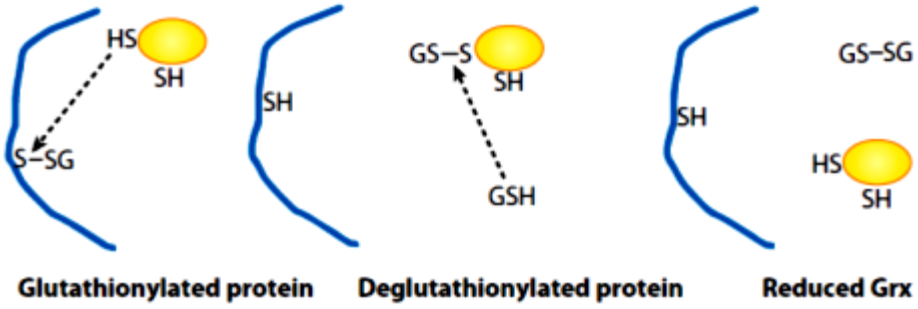

Figure 1.8. Deglutathionylation of a target protein by glutaredoxin (Grx). Reduced glutaredoxin (yellow circle) removes glutathione (GSH) from the glutathionylated protein and is subsequently reduced by GSH (Meyer *et al*., 2009).

This process of deglutathionylation is catalysed specifically by glutaredoxin in most organisms although it may also be catalysed by thioredoxins in yeast cells (Greetham *et al.*, 2010). Numerous dithiol glutaredoxins are capable of catalysing the GSH dependent reduction of disulfides or glutathionylated cysteines and are in turn reduced by GSH (Lillig *et al.*, 2008). As the glutathionylation/deglutathionylation cycle (Fig. 1.8) is a significant mechanism in redox regulation and signalling and (Allen and Mieyal, 2012), systems biology approaches need to be developed in order to accurately study the dynamics of the glutaredoxin system in context of cellular function.

1.4 Glutaredoxin dithiol and monothiol mechanisms in computational systems biology

Computational modelling of the glutaredoxin system may offer an invaluable method to understand the regulation of this system as a whole and may provide a guide for wet laboratory analyses as they provide mechanistic details and allow for the testing and refinement of hypotheses on redox mechanisms (Pillay *et al.*, 2013).

In any systems biology modelling approach the first step is to clearly define the components to be studied. It was however not instantly evident whether the redoxins should be modelled as redox couples or as enzymes in computational models (Pillay *et al.*, 2009). Redoxins could be modelled as redox couples as suggested by the use of redox potentials and ratios of oxidised to reduced redoxin to describe redoxins *in vivo* and *in vitro* (Aslund *et al.*, 1997). Alternatively, redoxin activity has been described using Michaelis-Menten kinetic parameters (Peltoniemi *et al.*, 2006; Gallogly *et al.*, 2008) suggesting that these redoxins could be modelled as enzymes. Recently, an analysis of the complete set of reactions in redoxin systems has provided a logical explanation for the discrepancies with the descriptions of redoxin activity presented in the literature. Using computational modelling, it was shown that redoxins should be accurately modelled as redox couples and that the enzymatic behaviour attributed to redoxins was due to saturation of the redox cycles within these systems (Pillay *et al.*, 2009). However, a number of additional inconsistencies with the description of these redoxin activities have made the systems biology analysis of these systems difficult (Pillay *et al.*, 2013).

For glutaredoxins particularly, two distinct mechanisms have been proposed in order to describe their activity using either one or both of the active site cysteines which make up the CxxC motif (Fig. 1.9). The monothiol mechanism requires only the N-terminal cysteine residue for the reduction of the GSH mixed disulfides whereas the dithiol mechanism proposes the use of both of the active site cysteine residues to reduce glutathionylated substrates. Interestingly, the dithiol mechanism is also used for the reduction of low molecular weight and protein disulfide substrates such as ribonucleotide reductase (Fig. 1.9; Yang and Wells, 1991; Bushweller *et al.*, 1992; Sagemark *et al.*, 2007).

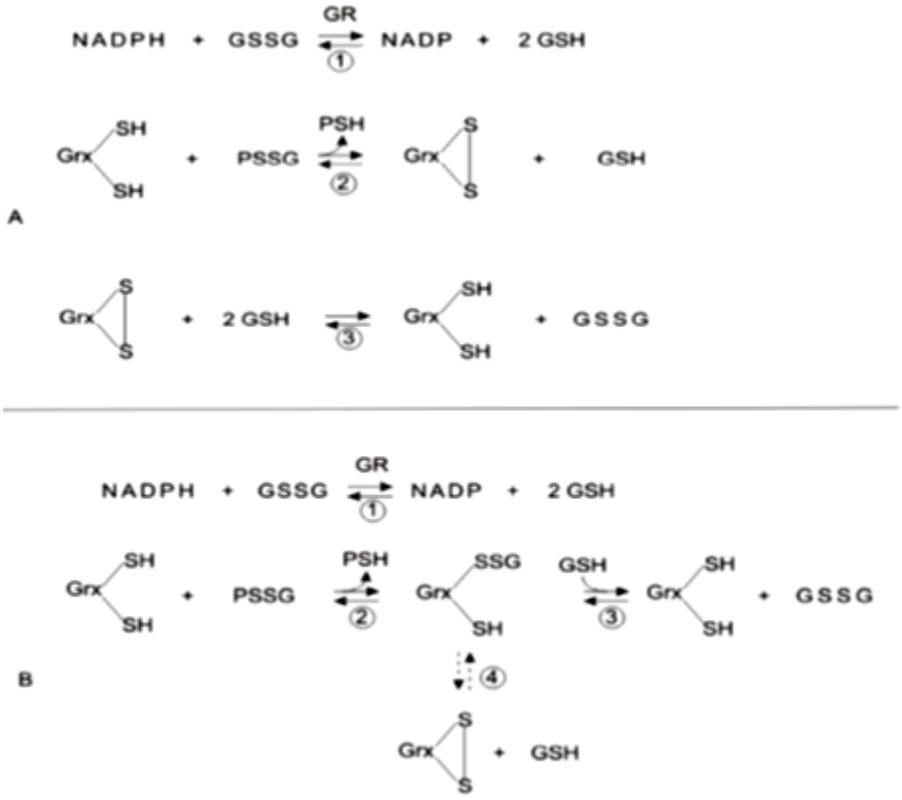

Figure 1.9. Proposed mechanisms for glutaredoxin activity showing the deglutathionylation of glutathionylated protein (PSSG) mixed disulfides catalysed by glutaredoxins. The dithiol mechanism (A) shows the reduction of the intramolecular disulfide (GrxSS) at the active site of the glutaredoxins by 2 GSH molecules forming glutathione disulfide (GSSG) and recycling the reduced glutaredoxin (Grx-S^-). The monothiol mechanism (B) shows the reduction of GrxSSG by GSH producing glutathione disulfide (GSSG) as the second product and recycling the reduced enzyme (Grx-S^-) is considered the rate-determining step. Shown in reaction 4 of this mechanism is a connected side reaction which includes the formation of the intramolecular disulfide (GrxSS) at the active site of the glutaredoxins (Mashamaite *et al.*, 2015).

A number of research efforts are focused on developing kinetic models of the glutaredoxin system (for example, Pillay *et al.*, 2009; Adimora *et al.*, 2010). However, models using either the monothiol and dithiol mechanism are expected to have different structural properties (Pillay *et al.*, 2013) due to the difference in GSH stoichiometry and species in both mechanisms (Fig. 1.10 A-C). These differences will result in computational models with different sets of ordinary differential equations (ODEs) (Fig 1.10D) and models based on either mechanism are therefore likely to produce different behaviours for the same set of input parameters (Pillay *et al.*, 2013). Resolving which mechanism should be used in computational models is the focus of this thesis.

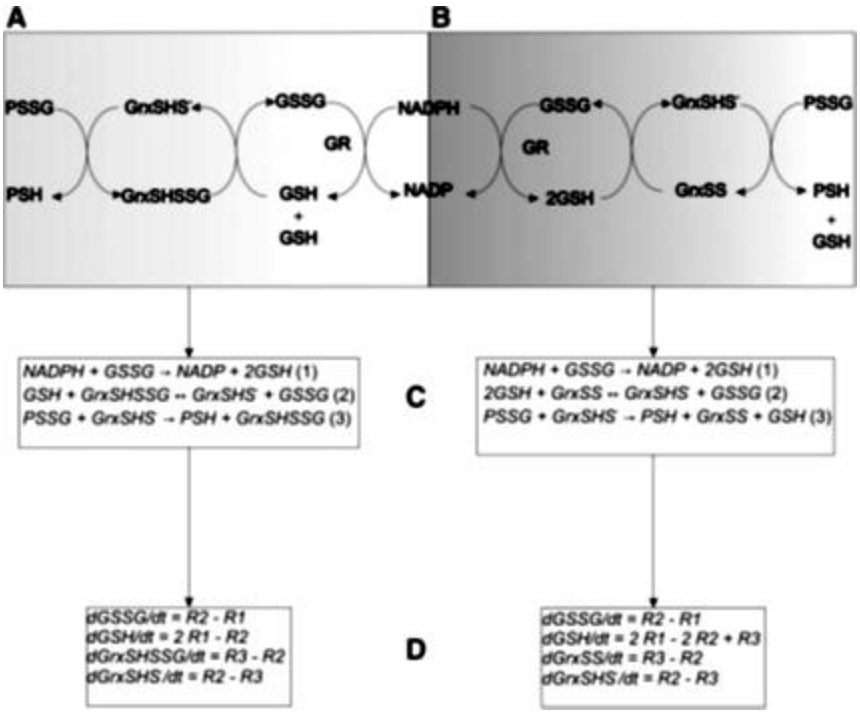

Figure 1.10. Proposed mechanisms for glutaredoxin activity. Depending on the mechanism, monothiol (A) or dithiol (B), the computational models based on these mechanisms will include either the GrxSHSSG/GrxSSG or GrxSS species (C), resulting in distinct sets of ordinary differential equations for these mechanisms (D) (Pillay *et al.*, 2013).

1.5 Discussion

Normal cellular processes cause the formation of reactive oxygen species, resulting in oxidative stress which may have negative effects on the cell and the organism as a whole. Many diseases such as cancer and Alzheimer's disease are caused or aggravated by oxidative stress (Cooke *et al.*, 2003). Cells have therefore developed non-redoxin and redoxin antioxidants in order to counteract the effects of oxidative stress. Redoxins in particular are very important as they are also responsible for the regulation of other processes within the cell (Storr *et al.*, 2013). For instance, by regulating hydrogen peroxide levels in the cytosol, peroxiredoxins regulate cell signalling and differentiation. Thioredoxins and glutaredoxins are necessary for the reduction of numerous proteins and play an important role in DNA synthesis (Toledano *et al.*, 2007; Du *et al.*, 2013)

Redox regulation is essential in cellular signalling and the changes in the redox state may lead to specific reversible oxidative modifications of important proteins (Jones, 2002, 2006). The glutathionylation of proteins under conditions where the GSH:GSSG ratio is decreased, is both a protective and regulatory mechanism (Ruoppolo *et al.*, 1997). Deglutathionylation seems to be generally mediated by glutaredoxins (Zaffagnini *et al.*, 2012) and is catalysed using one of two distinct mechanisms. In order to describe the dynamics of the GSH/glutaredoxin system using computational systems biology tools, we had to analyse the proposed mechanisms for deglutathionylation and determine which mechanism should be used in computational models. This basic research study can be used as a foundation to describe the roles played by glutaredoxin networks in a number of pathologies including cancer, and *Mycobacterium tuberculosis* and HIV infections (Gallogly and Mieyal, 2007).

Chapter 2: Additional discrepancies in the description of glutaredoxin deglutathionylation kinetics

In addition to the differences between the monothiol and dithiol mechanisms (see Figure 1.9), a number of other discrepancies for the glutaredoxins activity have been reported in the literature and are described below.

2.1 Discrepancy I: Activity of the Cxx(C→S) mutant

In theory, a glutaredoxin Cxx(C→S) mutant in which one of the active site cysteines is mutated to a serine could provide a good test system for determining protein disulfide reduction mechanism and distinguishing between the monothiol and dithiol mechanisms as this mutant is unable to form an intramolecular disulfide (GrxSS), which is a major intermediate of the dithiol mechanism (Bushweller *et al.*, 1992; Peltoniemi *et al.*, 2006). Kinetic analysis showed that such mutants were inactive as hydrogen donors for ribonucleotide reductase (Bushweller *et al.*, 1992) confirming that disulfide reduction follows a dithiol mechanism. However, the deglutathionylation activity data for these mutants was not as clear, as both higher and lower activities in the reduction of mixed disulfides have been reported.

An *E. coli* glutaredoxin Cxx(C→S) mutant was used in the β-hydroxyethyl disulfide (HEDS) assay to measure GSH-dependent glutaredoxin activity. The HEDS or β-mercaptoethanol (β-ME) disulfide assay is widely used to determine the specific activity of glutaredoxins (Holmgren, 1979a; Luikenhuis *et al.*, 1998). In this assay GSH spontaneously reduces HEDS and yields β-ME as well as a mixed disulfide between β-ME and GSH (β-ME-SG) (Lillig *et al.*, 2008; Li *et al.*, 2010). The addition of glutaredoxin to the β-ME-SG assay allows for reduction, resulting in β-ME and the formation of GrxSSG mixed disulfide. β-ME-SG is then reduced using a monothiol or a dithiol mechanism (Lillig *et al.*, 2008). The *E. coli* Cxx(C→S) glutaredoxin mutant retained only about 38% of the wild type glutaredoxin activity in the HEDS assay. Thus, in order for this glutaredoxin to be an effective reductant of glutathionylated substrates both active site cysteines were required (Bushweller *et al.*, 1992; Xiao *et al.*, 2005). Further, other investigations also showed that the wild type *E. coli* glutaredoxin had a higher reductase activity than the corresponding mutant glutaredoxin for

the reduction of an RNase-SG mixed disulfide (Xiao *et al.*, 2005). Similar results were reported with yeast glutaredoxin (Discola *et al.*, 2009).

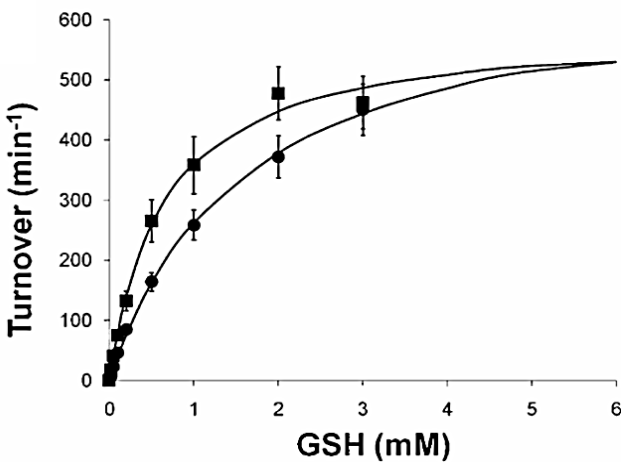

Figure 2.1. Comparison of mammalian wild type (●) and mutant (■) glutaredoxin activity using cysteine-glutathione disulfide (CSSG) (Gallogly *et al.*, 2008). (Permission to reproduce this figure was granted by American Chemical Society)

In contrast, a mammalian Grx2 mutant for was shown to have an enhanced deglutathionylation activity compared to wild-type Grx2 when cysteine-glutathione disulfide (CSSG) was used as a substrate. The result showed that only the N-terminal cysteine residue was necessary in this reaction and that the formation of the glutaredoxin disulfide detracted from catalysis (Fig. 2.1; Gallogly *et al.*, 2008). An interesting observation from these studies was that as GSH concentration increased the turnover of the wild type glutaredoxins became equal to that of the mutant (Fig. 2.1; Gallogly *et al.*, 2008). The reasons for these contradictory reports for glutaredoxin mutant and wild-type activity had not been elucidated.

2.2 Discrepancy II: GSH stoichiometry

The mono- and di- thiol reaction schema for deglutathionylation suggested that the different GSH stoichiometry involved in both mechanisms could also be used to distinguish them (Fig. 1.9; Gallogly *et al.*, 2008). As the monothiol mechanism makes use of only one GSH molecule per reaction event, a linear response to the changes in GSH concentration would be expected. On the other hand, as the dithiol mechanism utilises two GSH molecules per reaction, a non-linear rate response to changes in GSH concentration would be expected.

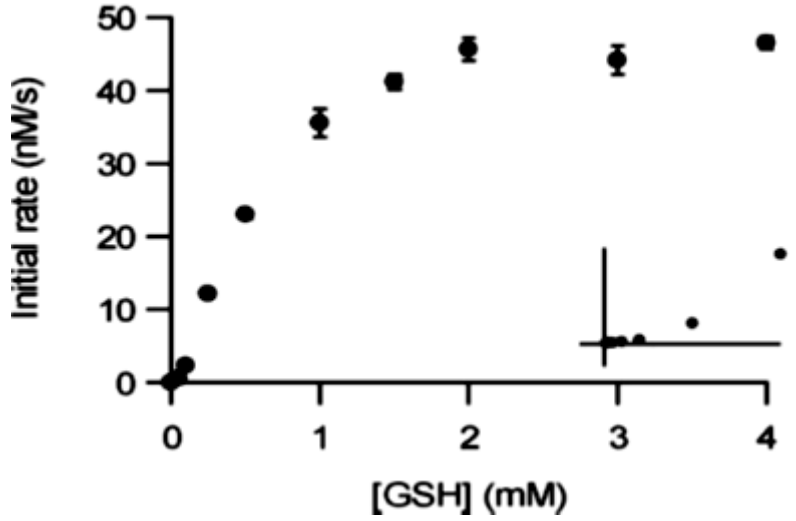

Figure 2.2. Analysis of changes in the rate of reaction of GSH concentration in glutaredoxin-catalysed peptide deglutathionylation in Escherichia coli with inset showing a Lineweaver-Burk plot of this reaction profile (Peltoniemi *et al.*, 2006). (Permission to reproduce this figure was granted by The American Society for Biochemistry and Molecular Biology)

In studies with *E. coli* Grx1 and a glutathionylated peptide, a sigmoidal increase was observed in the initial rate with increasing GSH concentrations and the resulting Lineweaver-Burk plot was non-linear and did not fit to the Michaelis-Menten equation, but instead showed a curved shape (Fig. 2.2; Peltoniemi *et al.*, 2006). A sigmoidal rate dependence on substrate concentration normally implies substrate co-operativity but is unlikely as the glutaredoxins are small molecules and have a single GSH binding site. These authors postulated that the sigmoidal shape was probably due to the effect of the Grx-GSH mixed disulfide intermediate alternating between the formation of reduced (GrxSH) or oxidised glutaredoxin (GrxSS) and the re-reduction of oxidised glutaredoxin by GSH. Interestingly oxidised glutaredoxin was a prominent species in quenched-flow experiments used to trap the deglutathionylation reaction intermediates in these experiments, and has been detected *in vivo* (Trotter and Grant, 2003; Peltoniemi *et al.*, 2006). Collectively, this observed kinetic pattern agreed with the expected pattern for the dithiol mechanism. However, others studies have indicated that deglutathionylation followed a linear dependence on GSH concentration (Mieyal *et al.*, 1991; Gallogly *et al.*, 2008).

2.3 Discrepancy III: Diagnostic kinetic patterns

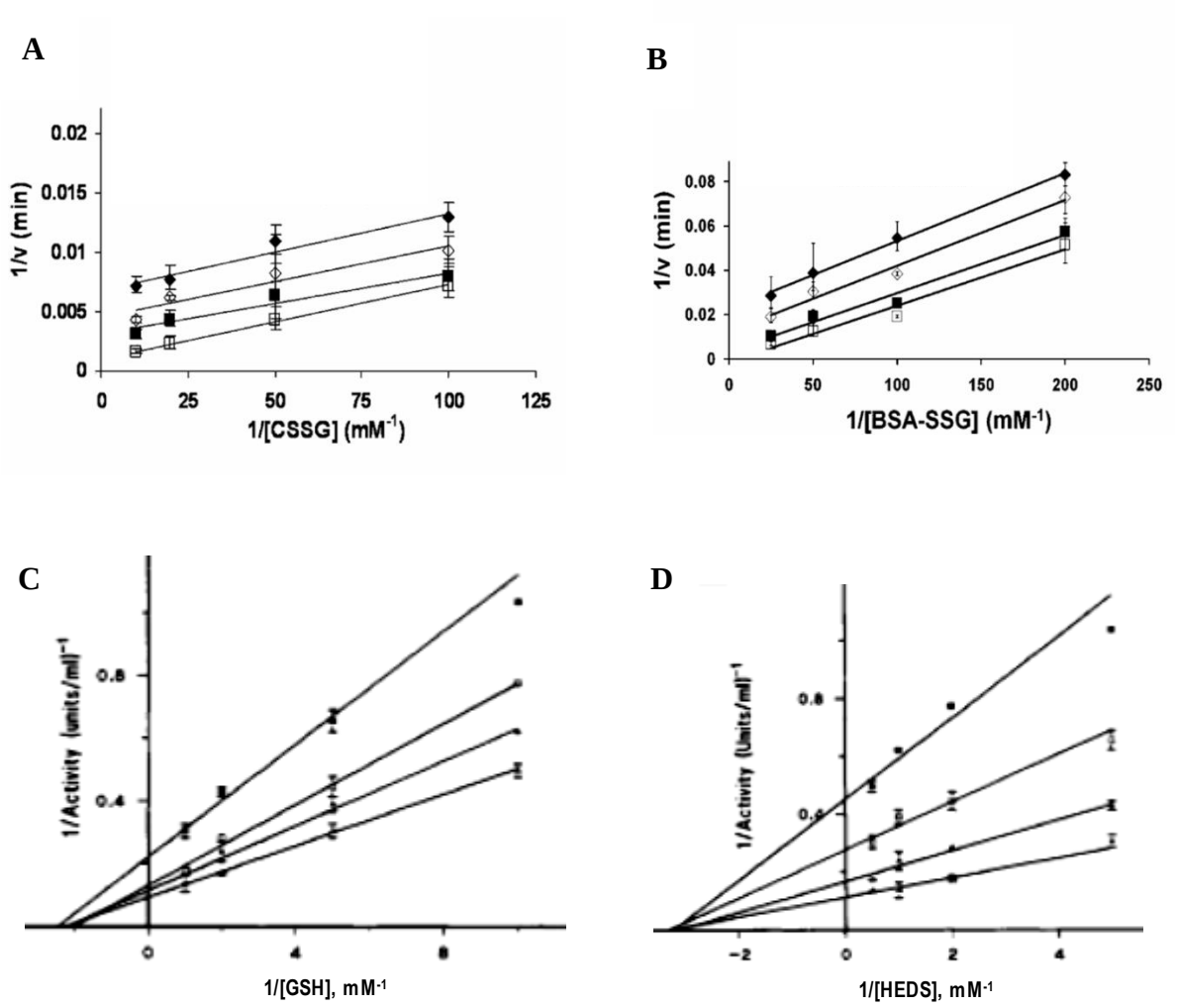

Figure 2.3. Different kinetic patterns for deglutathionylation were obtained with different substrates. Reciprocal plots for rate against changing concentration of CSSG and BSA-SSG showed ping-pong patterns (A and B) (Gallogly *et al.*, 2008) while a sequential pattern was obtained with the Lineweaver-Burk plots for GSH and HEDS (C and D) (Mieyal *et al.*, 1991). (Permission to reproduce these figures was granted by American Chemical Society)

The glutaredoxin-mediated thiol/disulfide exchange reactions involving the glutaredoxin/glutathione mixed disulfide (GrxSSG) was expected to give a ping-pong kinetic pattern because the data indicated that the reduction and oxidation of glutaredoxins occurred independently of each other (Gallogly *et al.*, 2009). This pattern was indeed observed in studies with the substrates CSSG and BSA-SSG (Fig. 2.3 A-B). However, studies revealed a sequential pattern where intersecting lines were obtained for both GSH and HEDS substrate

in double reciprocal plots (Fig 2.3 C-D; Mieyal *et al.*, 1991). It was proposed that these sequential patterns may occur as a result of simultaneous binding of GSH and glutaredoxin to the substrate, where preincubation of the substrate with GSH forms a glutathionylated substrate which is in turn reduced by the glutaredoxin (Mieyal *et al.*, 1991; Gravina and Mieyal, 1993; Mesecke *et al.*, 2008; Deponte, 2013). However, no data supporting this proposal has been produced.

2.4 Discussion

Apart from the structural differences in the mono- and di- thiol mechanisms (Table 2.1), a number of other inconsistencies exist in the literature on glutaredoxin activity, as summarised in the preceding sections. The discrepancies include the observed differences in the activity of the glutaredoxin mutant Cxx(C→S) compared to the wild type glutaredoxin (Mieyal *et al.*, 1991; Bushweller *et al.*, 1992; Gallogly *et al.*, 2008) and the observation of hyperbolic and sigmoidal patterns in kinetic rate plots resulting in both linear and curved line patterns in double reciprocal plots in response to GSH (Mieyal *et al.*, 1991; Peltoniemi *et al.*, 2006; Gallogly *et al.*, 2009). Additional discrepancies were also observed in the kinetic patterns, with two-substrate kinetic experiments showing both ping-pong and sequential kinetic patterns for glutathionylated substrates (Mieyal *et al.*, 1991; Gallogly *et al.*, 2009). It was therefore important to also resolve these discrepancies in addition to determining the mechanism used in the deglutathionylation process, before developing computational systems biology models of this particular system.

Table 2.1. Summary of differences in the dithiol and monothiol mechanisms.

Monothiol Mechanism	Dithiol Mechanism
• Cannot be used in catalysis of protein disulfide reduction. • Formation of the intramolecular disulfide (GrxSS) is a side reaction. • Changes in the rate of reaction with GSH concentration showed a linear response.	• Catalyses the reduction of protein disulfides. • Intramolecular disulfide (GrxSS) is central to catalysis. • Changes in the rate of reaction with GSH concentration showed a sigmoidal response.

Chapter 3: Resolving the discrepancies in the description of glutaredoxin kinetics with computational models

3.1 Introduction

As described in the previous chapter, the *in vitro* descriptions of the GSH/glutaredoxin system have resulted in discrepancies which have complicated the development of computational models for this system. The construction of kinetic models is progressively becoming more essential in redox biology for the quantification as well as for understanding the complexity of regulation of these systems in living cells (Pillay *et al.*, 2013). However, while computational and mathematical models are useful in describing complex biological systems, they can also be used to resolve discrepancies in kinetic data sets (Pillay *et al.*, 2013). In this section, we show how the GSH/glutaredoxin system can be accurately and consistently modelled.

3.2 Methods

3.2.1 Kinetic Modelling

Kinetic modelling experiments were carried out using the Python Simulator for Cellular Systems (PySCeS) (Olivier *et al.*, 2005). Previous studies from our group showed that the saturation of the redox cycles in the GSH/glutaredoxin system caused the enzyme-like behaviour attributed to glutaredoxins and that mass action kinetics was sufficient to describe the glutaredoxin activity (Pillay *et al.*, 2009). Therefore the glutaredoxin oxidation and reduction reactions were modelled using mass action kinetics while the glutathione reductase reaction was modelled with the irreversible form of a generic two-substrate rate expression (Rohwer *et al.*, 2006).

Core models with mass-action kinetics for the mono- and di- thiol mechanisms (Appendix 1; Pillay *et al.*, 2009) were parameterized using a basic kinetic parameter set to investigate the generic properties of these models (Table 3.1). Realistic models, incorporating realistic rate-expressions were parameterized using kinetic parameters from the BRENDA database (www.brenda-enzymes.org) or from the biochemical literature, and were fitted to *in*

vitro datasets using non-linear least squares regression with the Levenberg–Marquardt algorithm which is available through the SciPy library of scientific routines (http://www.scipy.org).

For the fitting experiments the dithiol mechanism was used to generate the model data (Appendix 1) which was fitted to *in vitro* datasets. The mono- and di- thiol mechanisms were modelled according to Fig 1.10 (C) with the models of these mechanisms having three reactions each. The first reaction for both mechanisms was the reduction of GSSG by glutathione reductase in the presence of NADPH, followed by the reduction of the intermediate GrxSSG by GSH in the monothiol mechanism or the reduction of oxidized glutaredoxin (GrxSS) in the dithiol mechanism. Both models included the deglutathionylation of a protein substrate (PSSG) by reduced glutaredoxin $(GrxSH)_2$. The purported side reaction involving oxidized glutaredoxin (GrxSS) in the monothiol mechanism was omitted from this model as it is not considered central to catalysis in this mechanism (Mieyal *et al.*, 2008; Deponte, 2013; Appendix 1).

3.3 Results

3.3.1 Computational models based on the dithiol and monothiol mechanisms give distinct results

Time course simulations were undertaken to analyse the changes in species concentration over time for both the monothiol and dithiol models using realistic parameter values (Gallogly *et al.*, 2008; Table 3.1). The monothiol mechanism includes the side reaction forming the intramolecular glutaredoxin (GrxSS) therefore distinguishing it from the mutant mechanism which cannot go through this reaction. The side reaction was however not included in the monothiol model. These time course simulations showed that both the monothiol and dithiol models were able to reach a steady state. In the monothiol mechanism two GSH molecules are released by glutathione reductase but only one GSH molecule is consumed in the deglutathionylation reaction (Appendix 1).This imbalance was resolved by modelling one of the GSH molecules in the first reaction (Fig. 3.2) as a fixed species as it is released from substrate PSSG. This species was expected to be present in smaller quantities

in relation to the free GSH in *in vitro* assays and within the cell (Peltoniemi *et al.*, 2006; Gallogly *et al.*, 2008).

Table 3.1. Parameters and values for core monothiol and dithiol models used in the time course simulation experiments for the analysis of glutathione/glutaredoxin systems.

	Values		Reference
	Monothiol	**Dithiol**	
Fixed Metabolites	**(µM)**	**(µM)**	
NADPH	200	200	Gallogly *et al.*, 2008
NADP	1	1	Gallogly *et al.*, 2008
PSSG	40	40	Gallogly *et al.*, 2008
PSH	1	1	Gallogly *et al.*, 2008
GSHp	-	1	
Variable Species	**(µM)**	**(µM)**	
GSH	500	998	Gallogly *et al.*, 2008
GSSG	500	1	Gallogly *et al.*, 2008
$Grx(SH)_2$	0.0675	0.0675	Gallogly *et al.*, 2008
GrxSS	-	0.0675	Gallogly *et al.*, 2008
GrxSSG	0.0675	-	Gallogly *et al.*, 2008
Kinetic Parameters			
K_{NADPH}	8 µM	8 µM	Worthington and Rosemeyer, 1976
K_{GSSG}	65 µM	65 µM	Worthington and Rosemeyer, 1976
k_{cat}	210 s^{-1}	210 s^{-1}	Worthington and Rosemeyer, 1976
k_2	$5.12e^{-5}$	$5.12e^{-5}$	-
k_3	0.054	0.054	-
[Glutathione reductase]	0.02 µM	0.02 µM	Gallogly *et al.*, 2008

Similarly, the dithiol mechanism showed that two GSH molecules are also released by glutathione reductase and both molecules are used in the deglutathionylation reaction. However, a further GSH molecule is liberated from the deglutathionylation of the substrate. This imbalance in this case was also resolved by modelling the GSH molecule liberated in this reaction as a fixed species GSHp (Fig 3.2). The time course simulations showed that the

dithiol model was also able to achieve steady state (Fig. 3.1 B, D). Despite having the same input parameters these models gave different results, as discussed in chapter 1.

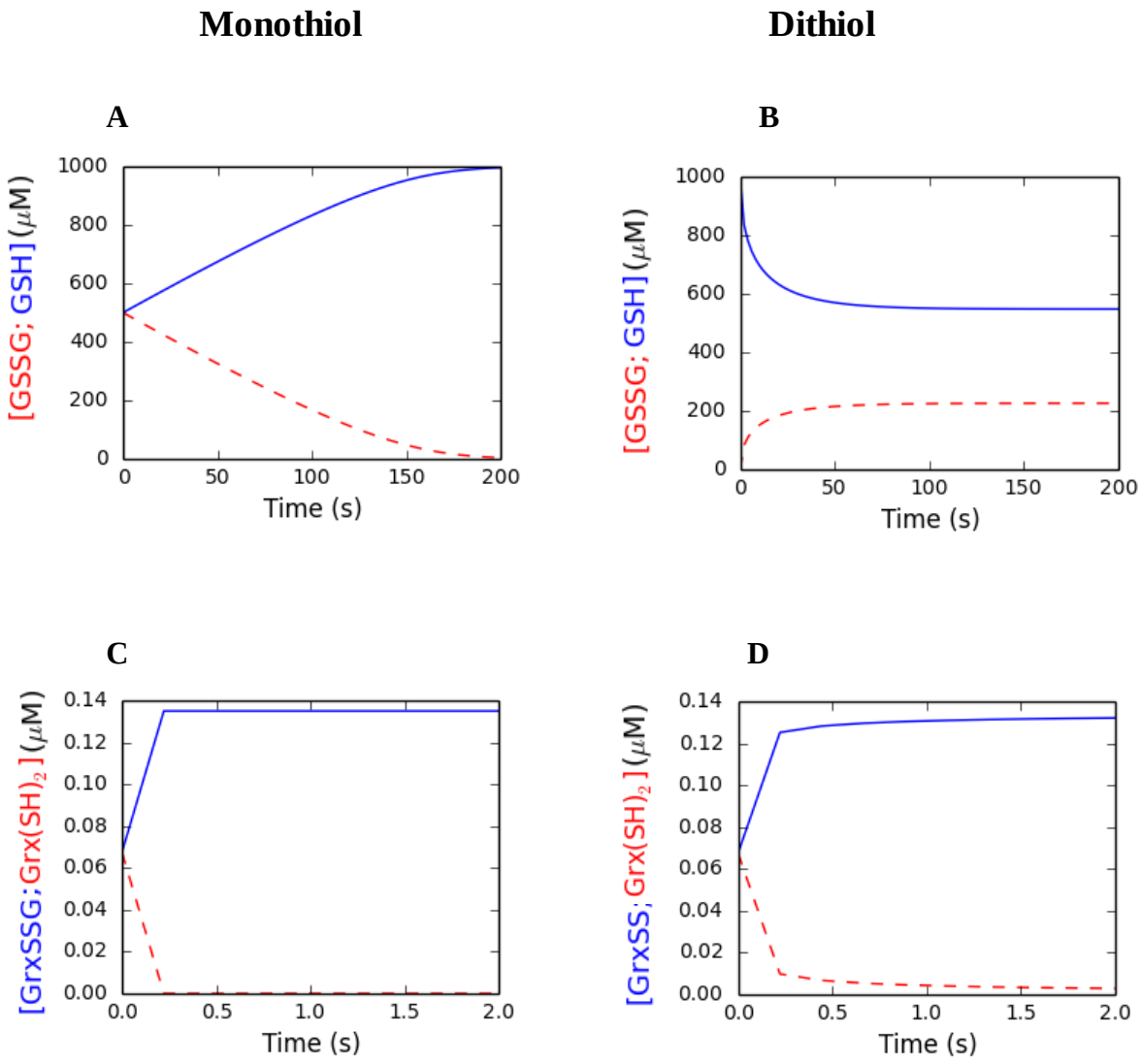

Figure 3.1. Time course simulations of the glutathione/glutaredoxin system using the monothiol (A and C) and dithiol (B and D) mechanisms with models of core parameter datasets (Table 3.1). Changes observed in the; GSH (solid line) and GSSG (Dashed line) (A), GrxSS (solid line) and GrxSH (dashed line) (B), GSH (solid line) and GSSG (Dashed line) (C), and GrxSSG (solid line) and GrxSH (dashed line) (D) over time.

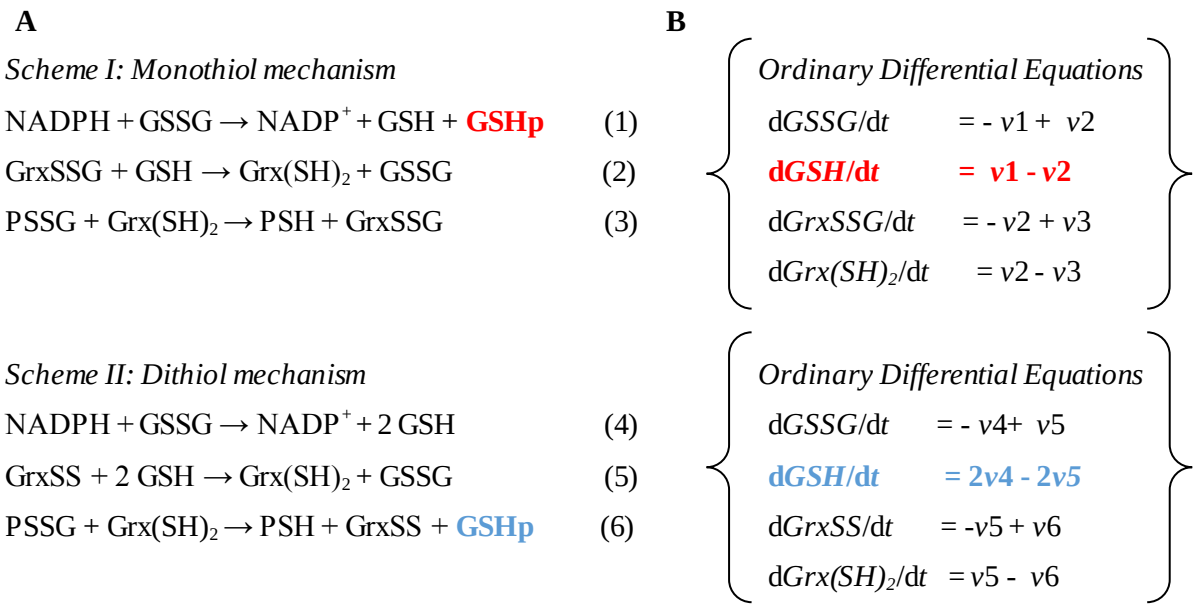

Figure 3.2. The dithiol and monothiol mechanisms (A) result in unbalanced ordinary differential equations (ODEs) (B). In the monothiol mechanism, the ODE for the glutathione moiety couple (GSH+GSSG) was balanced by modelling the GSH liberated from the substrate as GSHp in reaction (1) (Red) and the side reaction (GrxSSG → GrxSS + GSH) of the monothiol mechanism showing the formation of intramolecular glutaredoxin was not included in the model; in the dithiol mechanism the GSH liberated from the substrate is also treated as a separate species and modelled as GSHp in reaction (6) (Blue).

3.3.2 The dithiol and monothiol mechanisms are functionally equivalent

A central difference in the monothiol and dithiol mechanisms was the formation of a GrxSSG intermediate in the monothiol mechanism and not in the dithiol mechanism (Fig. 3.2). However, this mixed disulfide intermediate does feature in the dithiol mechanism if the reduction of the glutathionylated protein (PSSG) and reduction of oxidized glutaredoxin are carefully considered (Fig 3.3A). Another expected difference between the mechanisms was the formation of the intramolecular (GrxSS) disulfide, which was considered a side reaction in the monothiol mechanism but central to the dithiol mechanism (Fig 3.3B). However, once this side reaction was included in the monothiol mechanism, the two mechanisms were identical (Fig. 3.3), contrasting to the current literature on this system (see for example Gallogly *et al.*, 2008; Mieyal *et al.*, 2008; Deponte, 2013). While the oxidized glutaredoxin intermediate (GrxSS) has been detected in *in vitro* (Peltoniemi *et al.*, 2006) and *in vivo*

experiments (Trotter and Grant, 2003) GrxSSG could not be trapped in these experiments suggesting that it is a transient species and we will therefore not explicitly model it. The functional equivalence of the two mechanisms (Fig. 3.3) gave us a framework to tackle the other discrepancies in the description of deglutathionylation.

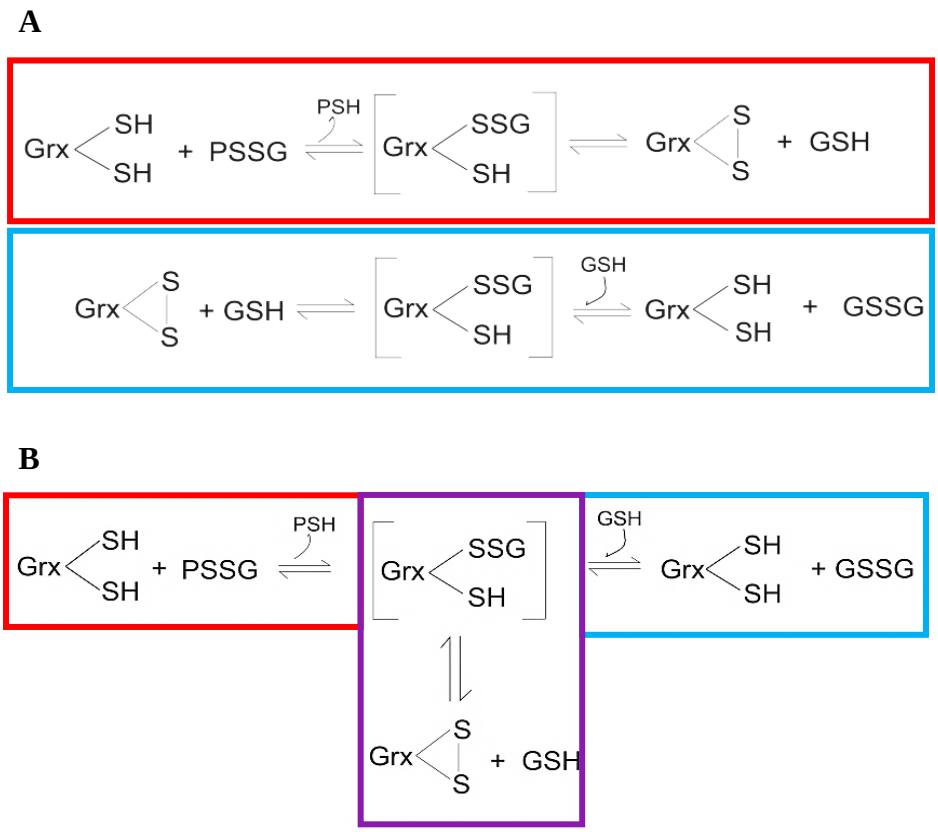

Figure 3.3. The proposed dithiol mechanism (A) is functionally equivalent to the monothiol mechanism (B). The deglutathionylation of PSSG mixed disulfides by reduced glutaredoxins $Grx(SH)_2$ showing the formation of the glutaredoxin mixed disulfide (GrxSSG) intermediate in both mechanisms (red) is followed by the reduction of oxidised glutaredoxin (GrxSS) by GSH (blue). The overlap of reactions (purple) occurs because the formation of the oxidised glutaredoxin (GrxSS) was considered as a side reaction in the monothiol mechanism.

3.3.3 Computational models of deglutathionylation can capture the *in vitro* kinetic behaviour accurately

On the basis that glutaredoxins were enzymes, a number of standard kinetic analyses of the GSH/glutaredoxin system have been undertaken. Michaelis-Menten parameters for glutaredoxin using glutathionylated substrates were determined using substrate saturation curves and Lineweaver-Burk reciprocal plots, and the effect of increasing glutaredoxin concentration on rate was also determined. In these analyses kinetic datasets were fitted to the Michaelis-Menten equation and the relevant K_m and k_{cat} parameters were determined (see for example Peltoniemi *et al.*, 2006; Gallogly *et al.*, 2008).

Computational experiments were therefore undertaken to see whether our dithiol core model with mass action kinetics could capture these *in vitro* kinetic behaviours (Fig. 3.4). In our modelling experiments, a classical saturation curve was observed for the substrate (PSSG) (Fig. 3.4 A). The initial rate of reaction for the substrate PSSG increased with the increasing concentration and thus the Lineweaver-Burk plot for PSSG reduction showed a linear dependence with increasing PSSG concentrations (Fig. 3.4 B). For the GSH saturation curve, the computational modelling results showed an increase in initial rate followed by saturation in the system (Fig 3.4 C). However the curve did not fit to the Michaelis-Menten equation and instead showed a curved line pattern in a Lineweaver-Burk plot (Fig. 3.4 D). This effect was postulated to be due to the net effect of the partitioning of the glutaredoxin-GSH mixed disulfide intermediate between the formation of reduced or oxidised glutaredoxins and the re-reduction of oxidised glutaredoxin by GSH (Peltoniemi *et al.*, 2006). However, this explanation was not clear and in our model, the sigmoidal dependencies of rate on GSH can be readily explained by the fact that two molecules of GSH are used for each reduction of oxidized glutaredoxin (GrxSS). Thus, the reaction order for this reaction is two (Equation 5; Scheme II, Fig 3.1). Finally there was a quasi-linear dependence of the initial deglutathionylation rate on the concentration of glutaredoxin (Fig. 3.4 E). Collectively these results showed that our computational modelling approach was consistent with the *in vitro* results obtained by Peltoniemi *et al.*, (2006) and Gallogly *et al.*, (2008).

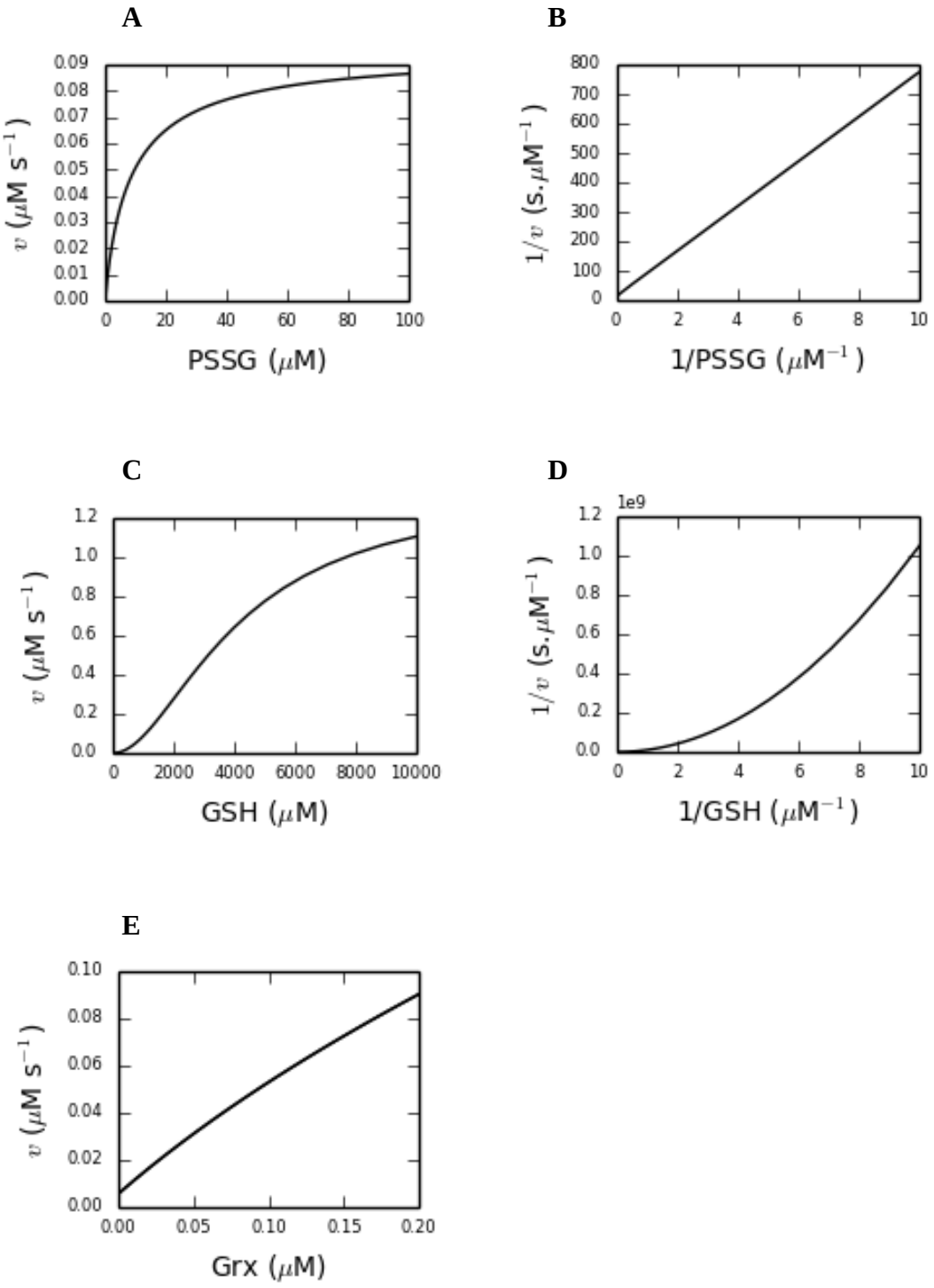

Figure 3.4. Analysis of kinetic behaviour of a realistic dithiol model (Table A1; Appendix 2) as a function of glutathionylated protein substrate (PSSG) (A) with the double-reciprocal Lineweaver-Burk plot for PSSG (B); as a function of the concentration of GSH (C) with the double-reciprocal Lineweaver-Burk plot (D); and as a function of the concentration of glutaredoxin (Grx) (E).

3.3.4 Grx Cxx(C→S) mutant and wild-type glutaredoxin kinetic studies showed that differences in activity is dependent on the rate of GSH oxidation

Core mathematical modelling was used to resolve the discrepancies in activities for reported wild type and mutant glutaredoxin. The dithiol mechanism (Scheme II) was used to represent the wild-type glutaredoxin with mass-action kinetics used to describe the reactions of this mechanism in the mathematical model (Pillay *et al.*, 2009).

To build this mathematical model, we focused on the reactions that showed the reduction of intramolecular disulfide (GrxSS) (equation 5) and the reduction of glutathionylated protein substrate (equation 6). The model consisted of a series of rate equations (equations 7-8) describing the kinetics of the glutaredoxin redox cycle (Scheme II; equations 7-8) and the sum of the glutaredoxin moiety couple (equation 9).

$$v_1 = k_1.PSSG.Grx(SH)_2 \quad (7)$$

$$v_2 = k_2.GrxSS.GSH^2 \quad (8)$$

$$Grx(SH)_2 + GrxSS = Grx_{tot} \quad (9)$$

At steady state $v_1 = v_2$, and therefore:

$$k_1.PSSG.Grx(SH)_2 = k_2.GrxSS.GSH^2 \quad (10)$$

Rearranging equation (10) yielded the following equation:

$$GrxSS = \frac{k_1.PSSG.Grx_{tot}}{k_1.PSSG + k_2.GSH^2} \quad (11)$$

Equation (11) was substituted into equation (10) to give the following expression for the rate of the wild-type (wt) mechanism:

$$v_{2wt} = \frac{PSSG.Grx_{tot}.GSH^2}{\frac{PSSG}{k_2}+\frac{GSH^2}{k_1}} = \frac{Grx_{tot}}{\frac{1}{k_2.GSH^2}+\frac{1}{k_1.PSSG}} \quad (12)$$

A similar set of equations was derived for the mutant. The reduction of the glutaredoxin mixed disulfide (GrxSSG) and the reduction of glutathionylated protein substrate were considered and the model consisted of a series of rate equations describing the

kinetics of these reactions. Equation (15) described the sum of the glutaredoxin moiety couple.

The reactions of the mutant mechanism were described by the following equations:

$$v_1 = k_1.PSSG.GrxSH \quad (13)$$

$$v_2 = k_2'.GrxSSG.GSH \quad (14)$$

$$GrxSSG + GrxSH = Grx_{tot} \quad (15)$$

The rate constants for the glutathione oxidation (v_2) are different for wild-type (k_2, $M^{-2}min^{-1}$) and mutant (k_2', $M^{-1}min^{-1}$) redoxins and were therefore not directly comparable.

Again, at steady state $v_1 = v_2$ and therefore:

$$k_1.PSSG.GrxSH = k_2'.GrxSSG.GSH \quad (16)$$

Rearranging equation (16) yielded equation (17):

$$GrxSSG = \frac{k_1.PSSG.Grx_{tot}}{k_1.PSSG + k_2'.GSH} \quad (17)$$

Equation (17) was substituted into equation (16) to give the following expression for the rate of the mutant (mu) mechanism:

$$v_{2mu} = \frac{PSSG.Grx_{tot}.GSH}{\frac{PSSG}{k_2'} + \frac{GSH}{k_1}} = \frac{Grx_{tot}}{\frac{1}{k_2'.GSH} + \frac{1}{k_1.PSSG}} \quad (18)$$

In order to compare the mechanisms, equation (12) could be divided by equation (18) yielding equation (19) which represents the ratio of the rates of the two mechanisms.

$$\frac{v_{2wt}}{v_{2mu}} = \frac{\frac{1}{k_2'.GSH} + \frac{1}{k_1.PSSG}}{\frac{1}{k_2.GSH^2} + \frac{1}{k_1.PSSG}} \quad (19)$$

The term $k_1.PSSG$ represents the reduction of the reduction of PSSG. For substrate concentrations that are high ($k_1.PSSG >> 1$), and equation (19) simplifies to:

$$\frac{v_{2wt}}{v_{2mu}} = \frac{k_2.GSH}{k_2'} \quad (20)$$

This simple mathematical model showed that at high substrate concentrations the difference in rate between the wild-type and mutant glutaredoxin can be described largely by the differences in the rate constants k_2 and k_2' for GSH oxidation. *In vitro* data by Srinivasan and colleagues (1997) showed that in glutaredoxin dependent reactions the GSH oxidation step is indeed the rate limiting step of the deglutathionylation reaction supporting our mathematical model. If the active site mutant has an increased rate constant for the oxidation of GSH ($k_2' > k_2\ GSH$), then the mutant could have higher activity compared to the wild type glutaredoxin. However, with increases in the glutathione concentration, equation (20) predicts that the relative rate of wild-type to mutant will increase. This has been confirmed by in vitro data with human Grx2 (cf. Fig. 2.2; Gallogly *et al.*, 2008) where mutant and wild-type rates became equivalent at high glutathione concentrations.

3.3.5 Reciprocal plot kinetics depend on the reversibility of the deglutathionylation reaction

Double-reciprocal kinetic plots for glutaredoxins have shown confusing data for deglutathionylation with some studies reporting a sequential mechanism while others have described a ping-pong mechanism. To understand this behaviour the standard ping-pong rate expression (equation 21) was compared to the rate expression for the wild-type glutaredoxin (equation 11) which was rearranged to give equation (22).

$$\frac{1}{v} = \frac{K_a}{V}\left(\frac{1}{a}\right) + \frac{1}{V}\left(\frac{K_b}{b} + 1\right) \tag{21}$$

$$\frac{1}{v_{2wt}} = \frac{k_1}{Grx_{tot}}\left(\frac{1}{PSSG}\right) + \frac{1}{Grx_{tot}.k_2}\left(\frac{1}{GSH^2}\right) \tag{22}$$

According to this analysis, the gradient of the line (k_1/Grx_{tot}, see equation 22) when plotting $1/v_{2\mathrm{wt}}$ against $1/PSSG$ is not affected by the changes in concentration of reduced glutathione (GSH). Therefore, the reciprocal plots of reaction rate against PSSG would result in a parallel line pattern (as normally observed for a ping-pong mechanism). However, in double reciprocal plots with GSH, a quadratic relationship would be expected.

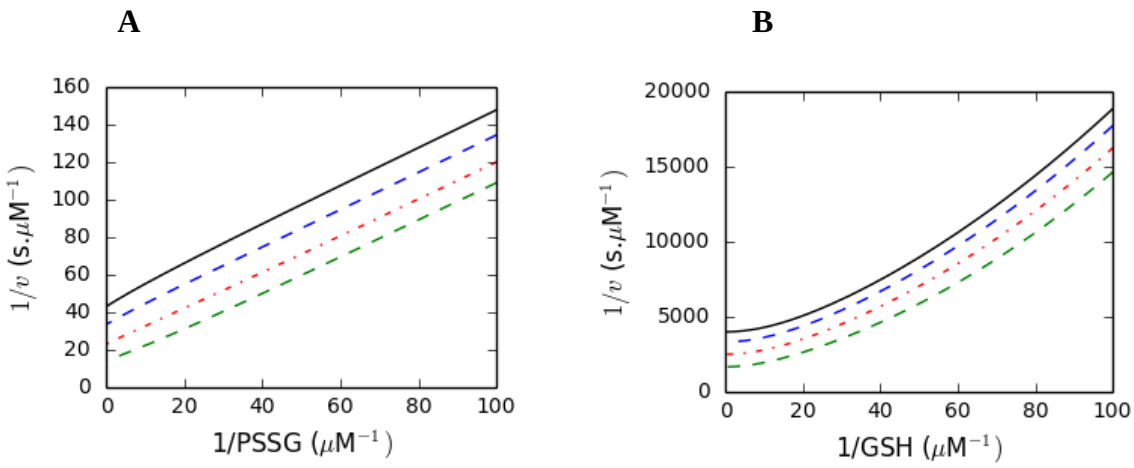

Figure 3.5. Two substrate kinetic pattern for a core dithiol model of glutaredoxin showing the dependence of glutaredoxin activity on glutathionylated substrate (PSSG) at various concentrations of GSH: black (0.25 µM) blue (0.30 µM) red (0.40 µM) and green (0.60 µM) (A), and the dependence of activity on GSH concentration at various concentrations of glutathionylated protein substrate (PSSG): black (0.00025 µM) blue (0.00030 µM) red (0.00040 µM) and green (0.00060 µM) (B).

To confirm this mathematical modelling result, reciprocal plot kinetics were obtained with the wild-type mechanism model. The expected ping pong kinetic pattern for the reciprocal plot showing rate against the reduction of glutathionylated protein substrate (PSSG) was indeed obtained (Fig. 3.5 A). The double reciprocal plot for GSH resulted in a curved line pattern (Fig 3.5 B) which was observed in the *in vitro* experiments (Peltoniemi *et al.*, 2006). However, a linear response of 1/*v* to 1/*GSH* was obtained in some two substrate kinetic *in vitro* studies (Mieyal *et al.*, 1991; Gallogly *et al.*, 2008). In these experiments only a few data points were used and the points chosen lay within the quasi-linear region of the curve (high $\frac{1}{GSH}$).

We next needed to determine the cause of the sequential pattern observed in some two substrate *in vitro* experiments. It was noted that the sequential patterns were observed in reciprocal plots where HEDS was used as a substrate. HEDS, as previously explained, reacts spontaneously with GSH forming the glutathionylated substrate β-ME-SG. However, in contrast to other glutathionylated substrates, the substrate can subsequently be reformed by the reaction of these products, and therefore this reaction was significantly reversible in the conditions described in these *in vitro* assays (Gravina and Mieyal, 1993). To investigate

whether this was important, the deglutathionylation reaction (reaction 6, Scheme II, Fig. 3.2), was modelled with reversible kinetics, using a K_{eq} value of one for the reduction of the glutathionylated substrate.

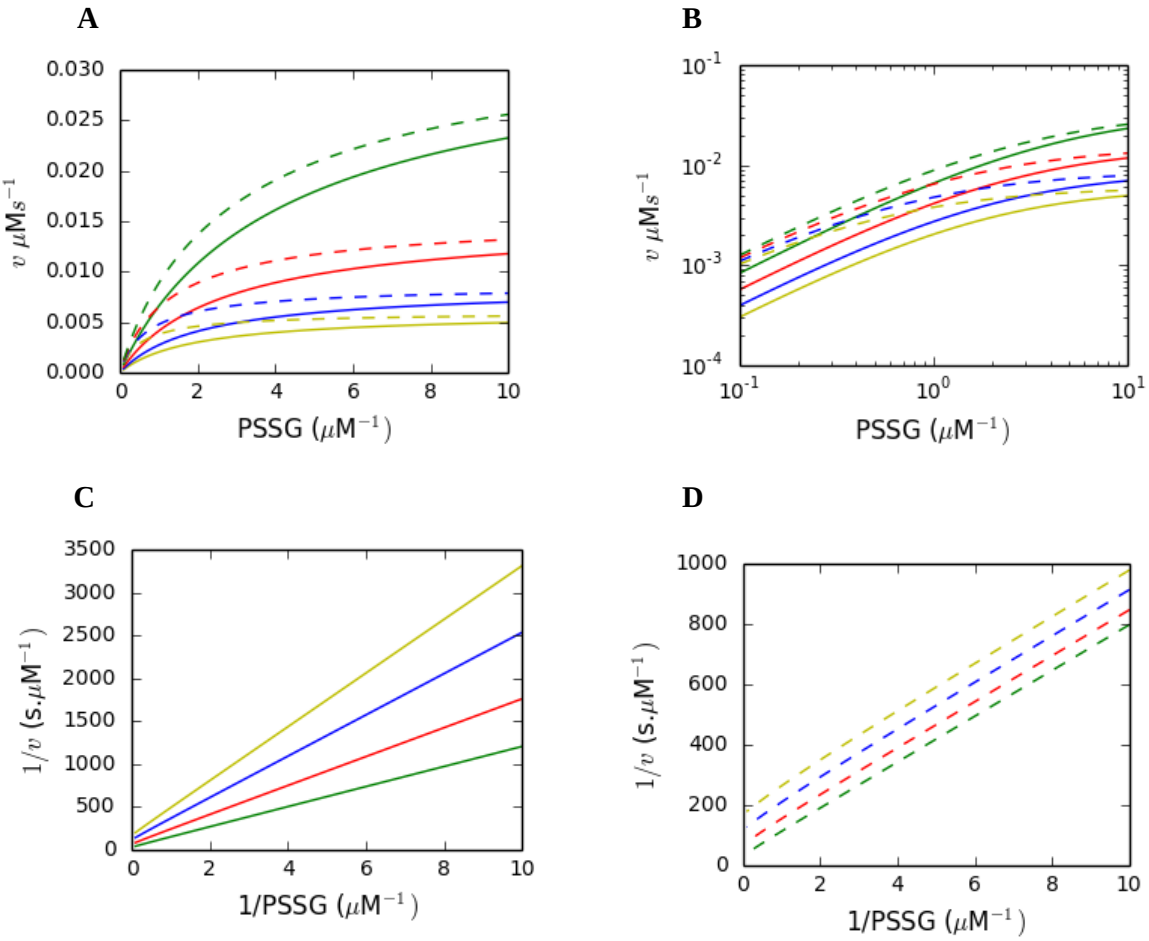

Figure 3.6. Two substrate kinetic experiments showing ping-pong and sequential patterns obtained for glutaredoxin dependent deglutathionylation reaction (Table A1; Appendix 2). The deglutathionylation reaction for fixed glutathionylated substrate (PSSG) at various concentrations of GSH, yellow (250 µM) blue (300 µM) red (400 µM) and green (600 µM) was modelled with reversible (solid) and irreversible (dashed) kinetic expressions (A), then a double log plot (B), and reciprocal plots (C-D) were generated for these different datasets.

When reversible and irreversible kinetics were compared (Fig. 3.6A), the differences in the initial reaction rates between increasing GSH concentrations and at lower PSSG concentrations were quiet significant (Fig.3.6B). The change from a reversible to an irreversible kinetic rate expression, led to change from a sequential pattern (Fig 3.6C), to the

observed ping-pong pattern (Fig. 3.6D). Our results showed that this resultant ping-pong pattern was due to the similarity of the initial rates of reaction for each PSSG concentration and thus when the reciprocal plot was generated, these rates shifted in such a way that the pattern showed parallel lines. On the other hand, with the use of the reversible kinetic rate expression the difference in the initial rate of reaction for each concentration of PSSG became exaggerated in the reciprocal plot (high 1/*PSSG*) which then resulted in the apparent sequential pattern, thus resolving this discrepancy in the literature.

3.3.6 Fitting *in vitro* datasets to the dithiol model

To further validate our dithiol kinetic modelling, several realistic *in vitro* kinetic datasets were fitted to a glutaredoxin model (Scheme II). The equilibrium constant (K_{eq}) for the reduction of the intramolecular glutaredoxin (GrxSS) in the dithiol mechanism (Appendix 1) was determined from the redox potentials of the glutaredoxin (-236mV) and GSH (-240mV) redox couples (Aslund *et al.*, 1997). The equilibrium constant for deglutathionylation of some of the substrates was unknown and so these reactions were modelled with irreversible kinetics.

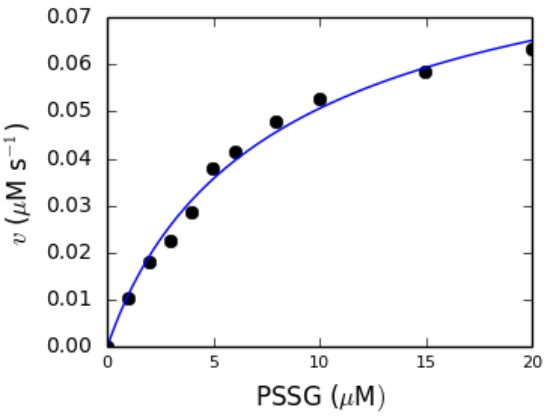

Figure 3.7. A kinetic model of the *Escherichia coli* glutaredoxin system (continuous line) was fitted on in vitro datasets (●) describing the deglutathionylation of a peptide (PSSG) (Peltoniemi *et al.*, 2006). The r^2 value was determined to be 0.990 with the rate constant for reduction of glutaredoxin by glutathione determined as $4.76 \times 10^{-06} \pm 2.99 \times 10^{-07}$ $\mu M^{-2}.s^{-1}$ and the rate constant for the reduction of PSSG by glutaredoxin determined as 0.66 ± 0.046 $\mu M^{-1}.s^{-1}$ (Appendix 2; Table A1).

The rate constants for the glutaredoxin system were determined by fitting the kinetic model to experimental datasets. For *E. coli* glutaredoxin, the kinetic model showed an excellent fit to a dataset describing reduction of a glutathionylated peptide substrate (PSSG) with an r^2 value of 0.990 (Fig. 3.7). The rate constants for PSSG reduction (k_3) was 0.66 ± 0.046 $\mu M^{-1}.s^{-1}$ while the rate constant for glutaredoxin reduction (k_2) was $4.76x10^{-06} \pm 2.99x10^{-07}$ $\mu M^{-2}.s^{-1}$

Fitting experiments were also done for yeast glutaredoxin using various *in vitro* datasets. We first fitted our kinetic model to datasets showing the reduction of HED with Grx1 and Grx2. The model fitted the data with r^2 values of 0.944 and 0.955 for Grx1 and Grx2 respectively (Fig. 3.8 A, B) with rate constants for Grx1 determined as $4.23x10^{-06} \pm 2.99x10^{-07}$ $\mu M^{-2}.s^{-1}$ and 0.07 ± 0.012 $\mu M^{-1}.s^{-1}$ for k_2 and k_3 respectively, and for Grx2, k_2 was $7.07x10^{-05} \pm 1.19x10^{-05}$ $\mu M^{-2}.s^{-1}$ and k_3 was 0.30 ± 0.057 $\mu M^{-1}.s^{-1}$. These results were not too surprising as these relatively lower r^2 values could be explained by the fact that in our model this reduction reaction was modelled with irreversible kinetics as the equilibrium constant for the reaction was not known.

We then looked at a different dataset which showed the change in the rate of oxidation of GSH by *S. cerevisiae* Grx1 with a HED substrate. This fitting experiment also showed a good fit with an r^2 value of 0.989 in the comparison between the model and the *in vitro* data (Fig. 3.8C; Discola *et al.*, 2009) with rate constants determined as $1.18x10^{-05} \pm 6.25x10^{-06}$ $\mu M^{-2}.s^{-1}$ and 0.26 ± 0.023 $\mu M^{-1}.s^{-1}$ for k_2 and k_3 respectively. The experiments with Grx1 should ideally show similar values for k_2, which is the rate constant for GSH oxidation. However, the predicted k_2 values for our fitting experiments were different and these differences may be due to the differences in the datasets. For example, the GSH dataset was obtained from a reciprocal plot in the literature therefore leading to exaggerated errors following the conversions of these points (Fig. 3.8 C). Collectively, these fitting experiments showed that the dithiol mechanism was sufficient for describing deglutathionylation.

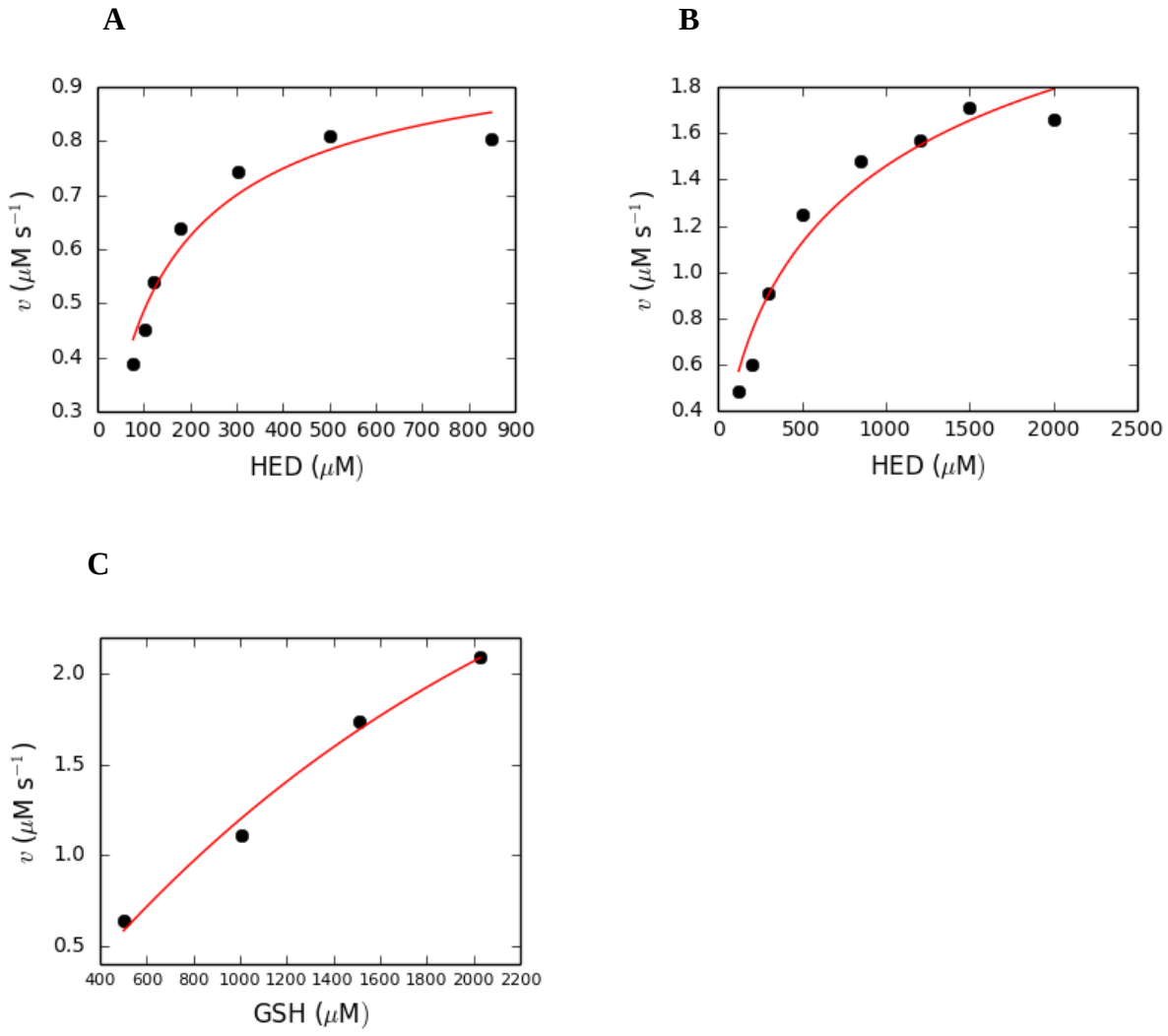

Figure 3.8. Comparison of the *Saccharomyces cerevisiae* kinetic model (continuous line) fitted to various in vitro (●) datasets. In (A), a Grx1 dithiol kinetic model was fitted to a HED dataset and the rate constants k_2 and k_3 were determined as $4.23 \times 10^{-06} \pm 2.99 \times 10^{-07}$ µM^{-2}.s^{-1} and 0.07 ± 0.012 µM^{-1}.s^{-1} respectively, while in (B) a Grx2 kinetic model was fitted to a HED dataset and the rate constants were determined as $k_2 = 7.07 \times 10^{-05} \pm 1.19 \times 10^{-05}$ µM^{-2}.s^{-1} and $k_3 = 0.30 \pm 0.057$ µM^{-1}.s^{-1} (Li *et al.*, 2010). When a Grx1 dithiol kinetic model was fitted to a GSH dataset with a HED substrate (Discola *et al.*, 2009) the rate constants k_2 and k_3 were determined as $1.18 \times 10^{-05} \pm 6.25 \times 10^{-06}$ µM^{-2}.s^{-1} and 0.26 ± 0.023 µM^{-1}.s^{-1} respectively (C) (Appendix 2, Table 2-3).

3.4 Discussion

Both the dithiol and monothiol mechanisms have been proposed for deglutathionylation, with data supporting both mechanisms presented in the literature. Deciding which mechanism should be used in computational systems biology models has therefore been difficult. Further, a number of other discrepancies have been reported *in vitro* kinetic studies (Chapter 2).

One of the major differences in the mono- and di- thiol mechanisms is that the GrxSSG mixed disulfide has been suggested to be the exclusive intermediate in the monothiol mechanism (Mieyal *et al.*, 2008). The monothiol mechanism also possesses a side reaction which includes the formation of the intramolecular disulfide GrxSS as another intermediate, which is assumed to detract from catalysis. Re-evaluation of both the dithiol and monothiol mechanisms showed that by including the side reaction in the monothiol mechanism and expanding the dithiol mechanism to include the transient GrxSSG mixed disulfide species in the basic structure of the mechanism, the two proposed mechanisms for deglutathionylation were identical (Fig. 3.3).

Considering the proposed functional equivalence of the two mechanisms, a computational dithiol model was considered sufficient in describing deglutathionylation for computational systems biology. It should be noted that the GrxSSG mixed disulfide was not included in this model because the partitioning to oxidised glutaredoxin (GrxSS) occurs rapidly as shown by trapping experiments (Peltoniemi *et al.*, 2006). This computational dithiol model was confirmed by our computational experiments which showed results consistent with the *in vitro* data presented in the literature (Fig. 3.4; Peltoniemi *et al.*, 2006) and was further able to fit a number of *in vitro* datasets. Furthermore, in a previous study, rate constants were determined for the deglutathionylation of PSSG by fitting kinetic model data to *in vitro* datasets reported by Peltoniemi *et al.*, (2006). This fitting experiment showed an extremely good fit with an r^2 value of 0.990 (Pillay *et al.*, 2009) and the dithiol model was able to successfully predict two independent datasets. The results from the fitting experiments shown in this thesis and from the previous study showed that the dithiol mechanism could be used to describe the GSH/glutaredoxin system in computational systems biology applications.

Mathematical models were used to describe the contrasting differences in the activity of the active site glutaredoxin mutant and native glutaredoxins. These results revealed the basis for the differences in the activity of the wild-type and mutant glutaredoxins. It was shown that the relative activities of the wild-type and mutant glutaredoxins depended on the rate constants for GSH oxidation and on GSH concentration. The mathematical model predicted that the activity of the mutant and wild-type glutaredoxins would become equivalent under conditions of increased GSH concentrations which was confirmed by *in vitro* kinetic data (cf. Fig. 2.2; Gallogly *et al.*, 2008).

Computational models also revealed a ping-pong kinetic pattern for the two substrate kinetic analysis of glutathionylated substrate (PSSG) as anticipated (Yang *et al.*, 1998). To understand the ping-pong behaviour, the standard ping-pong expression was compared to the kinetic rate expression determined or the wild-type glutaredoxin. It was shown that the gradient of the double-reciprocal plot for rate against PSSG was independent of the concentration of the substrate, which resulted in a characteristic ping-pong pattern (equation 22). However, the double-reciprocal plot for rate against GSH resulted in a non-linear relationship with a concavely curved dependence. This reciprocal plot showed a quadratic relationship with $1/GSH$ (equation 8), and thus at low concentrations of GSH (high $1/GSH$) these plots may appear linear, which was reported in some studies (Mieyal *et al.*, 1991; Gravina and Mieyal, 1993; Mieyal *et al.*, 1995; Gallogly *et al.*, 2008).

The literature also showed evidence of a sequential pattern when HEDS was used as a substrate for deglutathionylation (Mieyal *et al.*, 1991; Mieyal *et al.*, 1995). Our computational results showed that the sequential pattern was obtainable in a reciprocal plot if the reduction reaction of the substrate was modelled as a reversible reaction, providing a rational explanation in part for this effect. In conclusion we managed to resolve many of the discrepancies of the glutaredoxin activity described in the previous chapter and confirmed that the dithiol mechanism was sufficient in describing deglutathionylation in computational systems biology studies.

Chapter 4: General discussion and conclusion

Glutaredoxins are important electron donors found in most living cells. During their catalytic cycles glutaredoxins become oxidized and are reduced by glutathione (GSH) and glutathione reductase (GLR) which collectively form the GSH/glutaredoxin system. The GSH/glutaredoxin system is a major regulator of the redox state of a number of a number of processes such as DNA synthesis, iron metabolism and iron-sulfur cluster assembly (Berndt *et al.*, 2007). A key event in regulating the cellular response to oxidative stress is the formation of mixed disulfides between protein thiols and GSH in the glutathionylation process (Gravina and Mieyal, 1993). Numerous studies have shown that glutaredoxins can assist in the formation as well as the reduction of these mixed disulfides. Under normoxic conditions, the reduction of mixed disulfides is usually favoured, but under severe oxidative stress conditions the GSH:GSSG ratio is decreased and mixed disulfide formation is favoured (Beer *et al.*, 2004). Glutathionylation is also induced by mild oxidative stress and this process is an important redox regulatory mechanism (Ruoppolo *et al.*, 1997).

The kinetic mechanism of glutaredoxin dependent deglutathionylation was not clear as glutaredoxins had been proposed to follow either a mono- or a di-thiol mechanism (Bushweller *et al.*, 1992; Gallogly *et al.*, 2007; Mieyal *et al.*, 2008; Deponte, 2013). However, different structural properties were expected with computational systems biology models based on these mechanisms, and it was therefore likely that these models would produce different behaviours given the same set of input parameters. Moreover, the kinetic data supporting these mechanisms and describing glutaredoxin activity has also been extremely contradictory.

Several studies have attempted to explain the discrepancies in the description of the mechanism for deglutathionylation (Mieyal *et al.*, 2008; Gallogly *et al.*, 2009; Deponte, 2013). According to Deponte (2013) the dithiol and monothiol mechanisms cannot resolve these discrepancies of glutaredoxin activity. Consequently, two additional mechanisms were proposed, namely the glutathione scaffold model, which could explain why the monothiol glutaredoxins lacking activity in the HEDS assay were easily glutathionylated. The second model is the glutathione activator model which proposes an explanation for the sequential

kinetic pattern with the HEDS assay (Deponte, 2013). The suggested models were however very confusing and no data was provided for these mechanisms.

Using computational and mathematical models we were able to resolve these discrepancies. Firstly, and in contrast to the current thinking in this field, we showed that the mono- and di- thiol mechanisms were equivalent. Using a mathematical model we showed that the relative activity of mutant and wild-type glutaredoxins depended critically on the rate constant for GSH-oxidation and on the GSH concentration used in kinetic assays, which agreed with *in vitro* data (Srinivasan *et al.*, 1997; Gallogly *et al.*, 2009). To understand the contrasting reciprocal plot kinetics for glutaredoxins the mathematical model was modified and compared to the standard ping-pong kinetic expression. The results showed that a parallel line pattern was expected with a glutathionylated substrate but a curved line pattern would be obtained with increasing GSH concentrations. Kinetic modelling experiments also showed that a sequential pattern was obtainable when the reduction of the protein substrate was modelled with reversible kinetics. Collectively, these results together with the fitting experiments showed how deglutathionylation should be described in computational systems biology models.

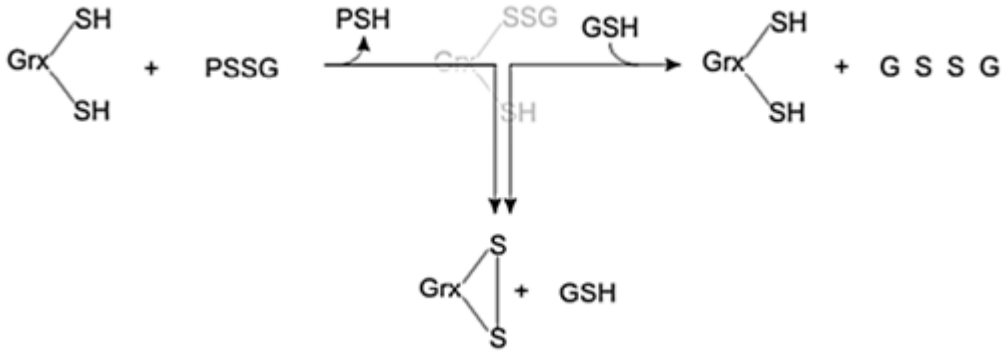

Figure 4.1. The formation of oxidized glutaredoxin in the presence of ROS may be a mechanism to prevent deglutathionylation by inactivating the glutaredoxin temporarily until activity is required (Mashamaite *et al*., 2015).

The kinetic mechanism revealed a potentially interesting aspect of glutaredoxin regulation and our results support a previous study by Peltoniemi *et al.* (2006). In this study it was proposed that the intramolecular disulfide formation between the two cysteines of the active site of glutaredoxins protects these thiols against hyper-oxidation (Peltoniemi *et al.*, 2006). Under oxidative stress conditions the GSH/GSSG ratio decreases (Zitka *et al.*, 2012),

this would leave the glutaredoxin trapped in the intramolecular disulfide (GrxSS) form. Once the stress was relieved, cellular GSH levels would increase and therefore active glutaredoxins will become available (Peltoniemi *et al.*, 2006). We suggest that the formation of this oxidized glutaredoxin under relatively high GSSG and low GSH concentrations (Peltoniemi *et al.*, 2006) temporarily inactivates glutaredoxins, preventing deglutathionylation under oxidative stress conditions. Protein thiols which are glutathionylated are therefore not prematurely exposed to ROS. This potential regulatory mechanism for glutaredoxin activity shows that the formation of the oxidised glutaredoxin (GrxSS) (Fig. 4.1) may be an important cellular redox sensor and may therefore be used as a biomarker for oxidative stress. This biomarker has an advantage over GSH/GSSG measurements as it may be less affected by compartment mixing during cell lysis (Morgan *et al.*, 2013).

In summary, these results have shown that considering the dynamics of the glutaredoxin system as a whole, allows for better prediction of kinetic regulatory behaviours. It is anticipated that the computational modelling presented in this thesis will play an important part in further describing the dynamic behaviours of the glutaredoxin system. Having identified the mechanism that should be used in computational systems biology enables us to model and analyse glutathionylation and deglutathionylation in various systems. For example human Grx1 has been suggested to protect the endothelial cells against oxidative stress because its expression was found to be elevated in coronary arteries in normal and atherosclerotic vessels (Adluri *et al.*, 2012) and Grx1 has also been shown to reduce the oxidant-induced cell death and apoptosis (Adluri *et al.*, 2012). Glutathionylation has also been recognised as a signalling mechanism in cardiovascular disease and a number of studies have shown the importance of oxidative cysteine changes in controlling cardiovascular function (Pastore and Piemonte, 2013) but, the mechanism linking the inhibition of oxidative stress and the cardio-protective capabilities by Grx1 is unclear (Adluri *et al.*, 2012).

This regulatory mechanism proposed above (Fig. 4.1) could be used to analyse the cardiovascular system more effectively in order to understand the effects of ROS and redox imbalance contributing to the pathogenesis of many diseases occurring in the cardiovascular system as well as in many other systems (Hare and Stamler, 2005; Gallogly *et al.*, 2009). However, further work is required to develop assays for oxidised glutaredoxin (GrxSS) and establish whether this is a viable cellular marker for oxidative stress. Evaluating the formation of GrxSS *in vitro* and *in vivo* will allow us to confirm the proposed protective abilities of this

species under oxidative stress conditions. Additionally, knowing how to describe deglutathionylation in computational systems biology means we are now able to develop computational models of real systems, enabling us to complement proteomic redox studies (Fratelli *et al.*, 2002; Fratelli *et al.*, 2004; Rouhier *et al.*, 2004; Meyer *et al.*, 2009). This could give us deeper insights into the glutathionylation/deglutathionylation cycle under physiological and pathophysiological conditions.

References

Adimora, N.J., Jones, D.P., Kemp, M.L., 2010. A model of redox kinetics implicates the thiol proteome in cellular hydrogen peroxide responses. Antioxidants & redox signaling 13, 731-743.

Adluri, R.S., Thirunavukkarasu, M., Zhan, L., Dunna, N.R., Akita, Y., Selvaraju, V., Otani, H., Sanchez, J.A., Ho, Y.S., Maulik, N., 2012. Glutaredoxin-1 overexpression enhances neovascularization and diminishes ventricular remodeling in chronic myocardial infarction. PloS one 7, e34790.

Akterin, S., Cowburn, R.F., Miranda-Vizuete, A., Jimenez, A., Bogdanovic, N., Winblad, B., Cedazo-Minguez, A., 2006. Involvement of glutaredoxin-1 and thioredoxin-1 in beta-amyloid toxicity and Alzheimer's disease. Cell Death Differ 13, 1454-1465.

Alam, Z.I., Jenner, A., Daniel, S.E., Lees, A.J., Cairns, N., Marsden, C.D., Jenner, P., Halliwell, B., 1997. Oxidative DNA damage in the parkinsonian brain: an apparent selective increase in 8-hydroxyguanine levels in substantia nigra. J Neurochem 69, 1196-1203.

Allen, E.M., Mieyal, J.J., 2012. Protein-thiol oxidation and cell death: regulatory role of glutaredoxins. Antioxidants & redox signaling 17, 1748-1763.

Aslund, F., Berndt, K.D., Holmgren, A., 1997. Redox potentials of glutaredoxins and other thiol-disulfide oxidoreductases of the thioredoxin superfamily determined by direct protein-protein redox equilibria. The Journal of biological chemistry 272, 30780-30786.

Aslund, F., Ehn, B., Miranda-Vizuete, A., Pueyo, C., Holmgren, A., 1994. Two additional glutaredoxins exist in Escherichia coli: glutaredoxin 3 is a hydrogen donor for ribonucleotide reductase in a thioredoxin/glutaredoxin 1 double mutant. Proceedings of the National Academy of Sciences of the United States of America 91, 9813-9817.

Bandyopadhyay, S., Starke, D.W., Mieyal, J.J., Gronostajski, R.M., 1998. Thioltransferase (glutaredoxin) reactivates the DNA-binding activity of oxidation-inactivated nuclear factor I. The Journal of biological chemistry 273, 392-397.

Barrett, W.C., DeGnore, J.P., Konig, S., Fales, H.M., Keng, Y.F., Zhang, Z.Y., Yim, M.B., Chock, P.B., 1999. Regulation of PTP1B via glutathionylation of the active site cysteine 215. Biochemistry 38, 6699-6705.

Beer, S.M., Taylor, E.R., Brown, S.E., Dahm, C.C., Costa, N.J., Runswick, M.J., Murphy, M.P., 2004. Glutaredoxin 2 catalyzes the reversible oxidation and glutathionylation of mitochondrial membrane thiol proteins: implications for mitochondrial redox regulation and antioxidant DEFENSE. The Journal of biological chemistry 279, 47939-47951.

Berndt, C., Lillig, C.H., Holmgren, A., 2007. Thiol-based mechanisms of the thioredoxin and glutaredoxin systems: implications for diseases in the cardiovascular system. American journal of physiology. Heart and circulatory physiology 292, H1227-1236.

Bushweller, J.H., Aslund, F., Wuthrich, K., Holmgren, A., 1992. Structural and functional characterization of the mutant Escherichia coli glutaredoxin (C14----S) and its mixed disulfide with glutathione. Biochemistry 31, 9288-9293.

Butterfield, D.A., Perluigi, M., Sultana, R., 2006. Oxidative stress in Alzheimer's disease brain: new insights from redox proteomics. Eur J Pharmacol 545, 39-50.

Camier, S., Ma, E., Leroy, C., Pruvost, A., Toledano, M., Marsolier-Kergoat, M.C., 2007. Visualization of ribonucleotide reductase catalytic oxidation establishes thioredoxins as its major reductants in yeast. Free radical biology & medicine 42, 1008-1016.

Carmel-Harel, O., Storz, G., 2000. Roles of the glutathione- and thioredoxin-dependent reduction systems in the Escherichia coli and saccharomyces cerevisiae responses to oxidative stress. Annu Rev Microbiol 54, 439-461.

Cencioni, C., Spallotta, F., Martelli, F., Valente, S., Mai, A., Zeiher, A.M., Gaetano, C., 2013. Oxidative stress and epigenetic regulation in ageing and age-related diseases. Int J Mol Sci 14, 17643-17663.

Chae, H.Z., Chung, S.J., Rhee, S.G., 1994. Thioredoxin-dependent peroxide reductase from yeast. The Journal of biological chemistry 269, 27670-27678.

Chen, J.W., Dodia, C., Feinstein, S.I., Jain, M.K., Fisher, A.B., 2000. 1-Cys peroxiredoxin, a bifunctional enzyme with glutathione peroxidase and phospholipase A2 activities. The Journal of biological chemistry 275, 28421-28427.

Chrestensen, C.A., Starke, D.W., Mieyal, J.J., 2000. Acute cadmium exposure inactivates thioltransferase (Glutaredoxin), inhibits intracellular reduction of protein-glutathionyl-mixed disulfides, and initiates apoptosis. The Journal of biological chemistry 275, 26556-26565.

Collinson, E.J., Wheeler, G.L., Garrido, E.O., Avery, A.M., Avery, S.V., Grant, C.M., 2002. The yeast glutaredoxins are active as glutathione peroxidases. The Journal of biological chemistry 277, 16712-16717.

Cooke, M.S., Evans, M.D., Dizdaroglu, M., Lunec, J., 2003. Oxidative DNA damage: mechanisms, mutation, and disease. FASEB journal : official publication of the Federation of American Societies for Experimental Biology 17, 1195-1214.

Dalle-Donne, I., Rossi, R., Colombo, G., Giustarini, D., Milzani, A., 2009. Protein S-glutathionylation: a regulatory device from bacteria to humans. Trends in biochemical sciences 34, 85-96.

Davis, D.A., Newcomb, F.M., Starke, D.W., Ott, D.E., Mieyal, J.J., Yarchoan, R., 1997. Thioltransferase (glutaredoxin) is detected within HIV-1 and can regulate the activity of glutathionylated HIV-1 protease in vitro. The Journal of biological chemistry 272, 25935-25940.

Dayer, R., Fischer, B.B., Eggen, R.I., Lemaire, S.D., 2008. The peroxiredoxin and glutathione peroxidase families in Chlamydomonas reinhardtii. Genetics 179, 41-57.

Declercq, J.P., Evrard, C., Clippe, A., Stricht, D.V., Bernard, A., Knoops, B., 2001. Crystal structure of human peroxiredoxin 5, a novel type of mammalian peroxiredoxin at 1.5 A resolution. Journal of molecular biology 311, 751-759.

Deponte, M., 2013. Glutathione catalysis and the reaction mechanisms of glutathione-dependent enzymes. Biochimica et biophysica acta 1830, 3217-3266.

Dexter, D.T., Wells, F.R., Lees, A.J., Agid, F., Agid, Y., Jenner, P., Marsden, C.D., 1989. Increased nigral iron content and alterations in other metal ions occurring in brain in Parkinson's disease. J Neurochem 52, 1830-1836.

Discola, K.F., de Oliveira, M.A., Rosa Cussiol, J.R., Monteiro, G., Barcena, J.A., Porras, P., Padilla, C.A., Guimaraes, B.G., Netto, L.E., 2009. Structural aspects of the distinct biochemical properties of glutaredoxin 1 and glutaredoxin 2 from Saccharomyces cerevisiae. Journal of molecular biology 385, 889-901.

Dixon, D.P., Davis, B.G., Edwards, R., 2002. Functional divergence in the glutathione transferase superfamily in plants. Identification of two classes with putative functions in redox homeostasis in Arabidopsis thaliana. The Journal of biological chemistry 277, 30859-30869.

Draculic, T., Dawes, I.W., Grant, C.M., 2000. A single glutaredoxin or thioredoxin gene is essential for viability in the yeast Saccharomyces cerevisiae. Molecular microbiology 36, 1167-1174.

Du, Y., Zhang, H., Zhang, X., Lu, J., Holmgren, A., 2013. Thioredoxin 1 is inactivated due to oxidation induced by peroxiredoxin under oxidative stress and reactivated by the glutaredoxin system. The Journal of biological chemistry 288, 32241-32247.

Eckers, E., Bien, M., Stroobant, V., Herrmann, J.M., Deponte, M., 2009. Biochemical characterization of dithiol glutaredoxin 8 from Saccharomyces cerevisiae: the catalytic redox mechanism redux. Biochemistry 48, 1410-1423.

Fernandes, A.P., Holmgren, A., 2004. Glutaredoxins: glutathione-dependent redox enzymes with functions far beyond a simple thioredoxin backup system. Antioxidants & redox signaling 6, 63-74.

Findlay, V.J., Tapiero, H., Townsend, D.M., 2005. Sulfiredoxin: a potential therapeutic agent? Biomed Pharmacother 59, 374-379.

Forman, H.J., Maiorino, M., Ursini, F., 2010. Signaling functions of reactive oxygen species. Biochemistry 49, 835-842.

Fratelli, M., Demol, H., Puype, M., Casagrande, S., Eberini, I., Salmona, M., Bonetto, V., Mengozzi, M., Duffieux, F., Miclet, E., Bachi, A., Vandekerckhove, J., Gianazza, E., Ghezzi, P., 2002. Identification by redox proteomics of glutathionylated proteins in oxidatively stressed human T lymphocytes. Proceedings of the National Academy of Sciences of the United States of America 99, 3505-3510.

Fratelli, M., Gianazza, E., Ghezzi, P., 2004. Redox proteomics: identification and functional role of glutathionylated proteins. Expert review of proteomics 1, 365-376.

Gallogly, M.M., Mieyal, J.J., 2007. Mechanisms of reversible protein glutathionylation in redox signaling and oxidative stress. Current opinion in pharmacology 7, 381-391.

Gallogly, M.M., Starke, D.W., Leonberg, A.K., Ospina, S.M., Mieyal, J.J., 2008. Kinetic and mechanistic characterization and versatile catalytic properties of mammalian glutaredoxin 2: implications for intracellular roles. Biochemistry 47, 11144-11157.

Gallogly, M.M., Starke, D.W., Mieyal, J.J., 2009. Mechanistic and kinetic details of catalysis of thiol-disulfide exchange by glutaredoxins and potential mechanisms of regulation. Antioxidants & redox signaling 11, 1059-1081.

Gelhaye, E., Rouhier, N., Jacquot, J.P., 2003. Evidence for a subgroup of thioredoxin h that requires GSH/Grx for its reduction. FEBS letters 555, 443-448.

Gella, A., Durany, N., 2009. Oxidative stress in Alzheimer disease. Cell Adh Migr 3, 88-93.

Gladyshev, V.N., Liu, A., Novoselov, S.V., Krysan, K., Sun, Q.A., Kryukov, V.M., Kryukov, G.V., Lou, M.F., 2001. Identification and characterization of a new mammalian glutaredoxin (thioltransferase), Grx2. The Journal of biological chemistry 276, 30374-30380.

Grant, C.M., 2001. Role of the glutathione/glutaredoxin and thioredoxin systems in yeast growth and response to stress conditions. Molecular microbiology 39, 533-541.

Gravina, S.A., Mieyal, J.J., 1993. Thioltransferase is a specific glutathionyl mixed disulfide oxidoreductase. Biochemistry 32, 3368-3376.

Greetham, D., Vickerstaff, J., Shenton, D., Perrone, G.G., Dawes, I.W., Grant, C.M., 2010. Thioredoxins function as deglutathionylase enzymes in the yeast Saccharomyces cerevisiae. BMC Biochem 11, 3.

Hanschmann, E.M., Godoy, J.R., Berndt, C., Hudemann, C., Lillig, C.H., 2013. Thioredoxins, glutaredoxins, and peroxiredoxins--molecular mechanisms and health significance: from cofactors to antioxidants to redox signaling. Antioxidants & redox signaling 19, 1539-1605.

Hare, J.M., Stamler, J.S., 2005. NO/redox disequilibrium in the failing heart and cardiovascular system. The Journal of clinical investigation 115, 509-517.

Herrero, E., de la Torre-Ruiz, M.A., 2007. Monothiol glutaredoxins: a common domain for multiple functions. Cell Mol Life Sci 64, 1518-1530.

Hirota, K., Matsui, M., Murata, M., Takashima, Y., Cheng, F.S., Itoh, T., Fukuda, K., Yodoi, J., 2000. Nucleoredoxin, glutaredoxin, and thioredoxin differentially regulate NF-kappaB, AP-1, and CREB activation in HEK293 cells. Biochemical and biophysical research communications 274, 177-182.

Hirotsu, S., Abe, Y., Okada, K., Nagahara, N., Hori, H., Nishino, T., Hakoshima, T., 1999. Crystal structure of a multifunctional 2-Cys peroxiredoxin heme-binding protein 23 kDa/proliferation-associated gene product. Proceedings of the

National Academy of Sciences of the United States of America 96, 12333-12338.

Holmgren, A., 1976. Hydrogen donor system for Escherichia coli ribonucleoside-diphosphate reductase dependent upon glutathione. Proceedings of the National Academy of Sciences of the United States of America 73, 2275-2279.

Holmgren, A., 1979a. Glutathione-dependent synthesis of deoxyribonucleotides. Characterization of the enzymatic mechanism of Escherichia coli glutaredoxin. The Journal of biological chemistry 254, 3672-3678.

Holmgren, A., 1979b. Glutathione-dependent synthesis of deoxyribonucleotides. Purification and characterization of glutaredoxin from Escherichia coli. The Journal of biological chemistry 254, 3664-3671.

Holmgren, A., 1984. Enzymatic reduction-oxidation of protein disulfides by thioredoxin. Methods in enzymology 107, 295-300.

Holmgren, A., 2000. Antioxidant function of thioredoxin and glutaredoxin systems. Antioxidants & redox signaling 2, 811-820.

Holmgren, A., Aslund, F., 1995. Glutaredoxin. Methods in enzymology 252, 283-292.

Holmgren, A., Lu, J., 2010. Thioredoxin and thioredoxin reductase: current research with special reference to human disease. Biochemical and biophysical research communications 396, 120-124.

Ito, H., Iwabuchi, M., Ogawa, K., 2003. The sugar-metabolic enzymes aldolase and triose-phosphate isomerase are targets of glutathionylation in Arabidopsis thaliana: detection using biotinylated glutathione. Plant Cell Physiol 44, 655-660.

Jacob, C., Holme, A.L., Fry, F.H., 2004. The sulfinic acid switch in proteins. Org Biomol Chem 2, 1953-1956.

Jones, D.P., 2002. Redox potential of GSH/GSSG couple: assay and biological significance. Methods in enzymology 348, 93-112.

Jones, D.P., 2006. Disruption of mitochondrial redox circuitry in oxidative stress. Chem Biol Interact 163, 38-53.

Kabore, A.F., Johnston, J.B., Gibson, S.B., 2004. Changes in the apoptotic and survival signaling in cancer cells and their potential therapeutic implications. Curr Cancer Drug Targets 4, 147-163.

Kalyanaraman, B., 2013. Teaching the basics of redox biology to medical and graduate students: Oxidants, antioxidants and disease mechanisms. Redox biology 1, 244-257.

Kim, K., Kim, I.H., Lee, K.Y., Rhee, S.G., Stadtman, E.R., 1988. The isolation and purification of a specific "protector" protein which inhibits enzyme inactivation by a thiol/Fe(III)/O2 mixed-function oxidation system. The Journal of biological chemistry 263, 4704-4711.

Klatt, P., Pineda Molina, E., Perez-Sala, D., Lamas, S., 2000. Novel application of S-nitrosoglutathione-Sepharose to identify proteins that are potential targets for S-nitrosoglutathione-induced mixed-disulphide formation. The Biochemical journal 349, 567-578.

Laurent, T.C., Moore, E.C., Reichard, P., 1964. Enzymatic Synthesis of Deoxyribonucleotides. Iv. Isolation and Characterization of Thioredoxin, the Hydrogen Donor from Escherichia Coli B. The Journal of biological chemistry 239, 3436-3444.

Li, W.F., Yu, J., Ma, X.X., Teng, Y.B., Luo, M., Tang, Y.J., Zhou, C.Z., 2010. Structural basis for the different activities of yeast Grx1 and Grx2. Biochimica et biophysica acta 1804, 1542-1547.

Lillig, C.H., Prior, A., Schwenn, J.D., Aslund, F., Ritz, D., Vlamis-Gardikas, A., Holmgren, A., 1999. New thioredoxins and glutaredoxins as electron donors of 3'-phosphoadenylylsulfate reductase. The Journal of biological chemistry 274, 7695-7698.

Lillig, C.H., Potamitou, A., Schwenn, J.D., Vlamis-Gardikas, A., Holmgren, A., 2003. Redox regulation of 3'-phosphoadenylylsulfate reductase from Escherichia coli by glutathione and glutaredoxins. The Journal of biological chemistry 278, 22325-22330.

Lillig, C.H., Berndt, C., Holmgren, A., 2008. Glutaredoxin systems. Biochimica et biophysica acta 1780, 1304-1317.

Lillig, C.H., Berndt, C., 2013. Glutaredoxins in thiol/disulfide exchange. Antioxidants & redox signaling 18, 1654-1665.

Lind, C., Gerdes, R., Hamnell, Y., Schuppe-Koistinen, I., von Lowenhielm, H.B., Holmgren, A., Cotgreave, I.A., 2002. Identification of S-glutathionylated cellular proteins during oxidative stress and constitutive metabolism by affinity

purification and proteomic analysis. Archives of biochemistry and biophysics 406, 229-240.

Lu, J., Holmgren, A., 2014. The thioredoxin antioxidant system. Free radical biology & medicine 66, 75-87.

Luikenhuis, S., Perrone, G., Dawes, I.W., Grant, C.M., 1998. The yeast Saccharomyces cerevisiae contains two glutaredoxin genes that are required for protection against reactive oxygen species. Molecular biology of the cell 9, 1081-1091.

Martin, J.L., 1995. Thioredoxin--a fold for all reasons. Structure 3, 245-250.

Mates, J.M., Perez-Gomez, C., Nunez de Castro, I., 1999. Antioxidant enzymes and human diseases. Clin Biochem 32, 595-603.

Mates, J.M., Sanchez-Jimenez, F.M., 2000. Role of reactive oxygen species in apoptosis: implications for cancer therapy. The international journal of biochemistry & cell biology 32, 157-170.

Mates, J.M., Segura, J.A., Alonso, F.J., Marquez, J., 2008. Intracellular redox status and oxidative stress: implications for cell proliferation, apoptosis, and carcinogenesis. Arch Toxicol 82, 273-299.

Mates, J.M., Segura, J.A., Alonso, F.J., Marquez, J., 2010. Roles of dioxins and heavy metals in cancer and neurological diseases using ROS-mediated mechanisms. Free radical biology & medicine 49, 1328-1341.

Mates, J.M., Segura, J.A., Alonso, F.J., Marquez, J., 2012. Oxidative stress in apoptosis and cancer: an update. Arch Toxicol 86, 1649-1665.

Melis, J.P., van Steeg, H., Luijten, M., 2013. Oxidative DNA damage and nucleotide excision repair. Antioxidants & redox signaling 18, 2409-2419.

Mesecke, N., Mittler, S., Eckers, E., Herrmann, J.M., Deponte, M., 2008. Two novel monothiol glutaredoxins from Saccharomyces cerevisiae provide further insight into iron-sulfur cluster binding, oligomerization, and enzymatic activity of glutaredoxins. Biochemistry 47, 1452-1463.

Meyer, Y., Buchanan, B.B., Vignols, F., Reichheld, J.P., 2009. Thioredoxins and glutaredoxins: unifying elements in redox biology. Annual review of genetics 43, 335-367.

Michelet, L., Zaffagnini, M., Marchand, C., Collin, V., Decottignies, P., Tsan, P., Lancelin, J.M., Trost, P., Miginiac-Maslow, M., Noctor, G., Lemaire, S.D.,

2005. Glutathionylation of chloroplast thioredoxin f is a redox signaling mechanism in plants. Proceedings of the National Academy of Sciences of the United States of America 102, 16478-16483.

Mieyal, J.J., Gallogly, M.M., Qanungo, S., Sabens, E.A., Shelton, M.D., 2008. Molecular mechanisms and clinical implications of reversible protein S-glutathionylation. Antioxidants & redox signaling 10, 1941-1988.

Mieyal, J.J., Srinivasan, U., Starke, D.W., Gravina, S.A., Mieyal, P.A. (Eds.), 1995. Glutathionyl specificity of the Thioltransferases: Mechanistic and Physiological Implications. Marcel Dekker, Inc;, New York.

Mieyal, J.J., Starke, D.W., Gravina, S.A., Hocevar, B.A., 1991. Thioltransferase in human red blood cells: kinetics and equilibrium. Biochemistry 30, 8883-8891.

Miranda-Vizuete, A., Damdimopoulos, A.E., Gustafsson, J., Spyrou, G., 1997. Cloning, expression, and characterization of a novel Escherichia coli thioredoxin. The Journal of biological chemistry 272, 30841-30847.

Miura, K., Fujibuchi, W., Ishida, K., Naitoh, T., Ogawa, H., Ando, T., Yazaki, N., Watanabe, K., Haneda, S., Shibata, C., Sasaki, I., 2011. Inhibitor of apoptosis protein family as diagnostic markers and therapeutic targets of colorectal cancer. Surg Today 41, 175-182.

Morgan, B., Ezerina, D., Amoako, T.N., Riemer, J., Seedorf, M., Dick, T.P., 2013. Multiple glutathione disulfide removal pathways mediate cytosolic redox homeostasis. Nature chemical biology 9, 119-125.

Muller, E.G.D., 1996. A glutathione reductase mutant of yeast accumulates high levels of oxidized glutathione and requires thioredoxin for growth. Molecular Biology of the Cell 7, 1805-1813.

Ogawa, K., Tasaka, Y., Mino, M., Tanaka, Y., Iwabuchi, M., 2001. Association of glutathione with flowering in Arabidopsis thaliana. Plant Cell Physiol 42, 524-530.

Olivier, B.G., Rohwer, J.M., Hofmeyr, J.H., 2005. Modelling cellular systems with PySCeS. Bioinformatics (Oxford, England) 21, 560-561.

Pastore, A., Piemonte, F., 2013. Protein glutathionylation in cardiovascular diseases. Int J Mol Sci 14, 20845-20876.

Peltoniemi, M.J., Karala, A.R., Jurvansuu, J.K., Kinnula, V.L., Ruddock, L.W., 2006. Insights into deglutathionylation reactions. Different intermediates in the

glutaredoxin and protein disulfide isomerase catalyzed reactions are defined by the gamma-linkage present in glutathione. The Journal of biological chemistry 281, 33107-33114.

Perry, T.L., Yong, V.W., 1986. Idiopathic Parkinson's disease, progressive supranuclear palsy and glutathione metabolism in the substantia nigra of patients. Neurosci Lett 67, 269-274.

Pillay, C.S., Hofmeyr, J.H., Mashamaite, L.N., Rohwer, J.M., 2013. From top-down to bottom-up: computational modeling approaches for cellular redoxin networks. Antioxidants & redox signaling 18, 2075-2086.

Pillay, C.S., Hofmeyr, J.H., Olivier, B.G., Snoep, J.L., Rohwer, J.M., 2009. Enzymes or redox couples? The kinetics of thioredoxin and glutaredoxin reactions in a systems biology context. The Biochemical journal 417, 269-275.

Prinz, W.A., Aslund, F., Holmgren, A., Beckwith, J., 1997. The role of the thioredoxin and glutaredoxin pathways in reducing protein disulfide bonds in the Escherichia coli cytoplasm. The Journal of biological chemistry 272, 15661-15667.

Proctor, P.H., Reynolds, E.S., 1984. Free radicals and disease in man. Physiol Chem Phys Med NMR 16, 175-195.

Raj, L., Ide, T., Gurkar, A.U., Foley, M., Schenone, M., Li, X., Tolliday, N.J., Golub, T.R., Carr, S.A., Shamji, A.F., Stern, A.M., Mandinova, A., Schreiber, S.L., Lee, S.W., 2011. Selective killing of cancer cells by a small molecule targeting the stress response to ROS. Nature 475, 231-234.

Rhee, S.G., Chae, H.Z., Kim, K., 2005. Peroxiredoxins: a historical overview and speculative preview of novel mechanisms and emerging concepts in cell signaling. Free radical biology & medicine 38, 1543-1552.

Rhee, S.G., Chang, T.S., Bae, Y.S., Lee, S.R., Kang, S.W., 2003. Cellular regulation by hydrogen peroxide. J Am Soc Nephrol 14, S211-215.

Rhee, S.G., Woo, H.A., Kil, I.S., Bae, S.H., 2012. Peroxiredoxin functions as a peroxidase and a regulator and sensor of local peroxides. The Journal of biological chemistry 287, 4403-4410.

Riederer, P., Sofic, E., Rausch, W.D., Schmidt, B., Reynolds, G.P., Jellinger, K., Youdim, M.B., 1989. Transition metals, ferritin, glutathione, and ascorbic acid in parkinsonian brains. J Neurochem 52, 515-520.

Rohwer, J.M., Hanekom, A.J., Crous, C., Snoep, J.L., Hofmeyr, J.H., 2006. Evaluation of a simplified generic bi-substrate rate equation for computational systems biology. Syst Biol (Stevenage) 153, 338-341.

Rouhier, N., Gelhaye, E., Jacquot, J.P., 2004. Plant glutaredoxins: still mysterious reducing systems. Cell Mol Life Sci 61, 1266-1277.

Ruoppolo, M., Lundstrom-Ljung, J., Talamo, F., Pucci, P., Marino, G., 1997. Effect of glutaredoxin and protein disulfide isomerase on the glutathione-dependent folding of ribonuclease A. Biochemistry 36, 12259-12267.

Russel, M., Model, P., Holmgren, A., 1990. Thioredoxin or glutaredoxin in Escherichia coli is essential for sulfate reduction but not for deoxyribonucleotide synthesis. Journal of bacteriology 172, 1923-1929.

Sagemark, J., Elgan, T.H., Burglin, T.R., Johansson, C., Holmgren, A., Berndt, K.D., 2007. Redox properties and evolution of human glutaredoxins. Proteins 68, 879-892.

Saggu, H., Cooksey, J., Dexter, D., Wells, F.R., Lees, A., Jenner, P., Marsden, C.D., 1989. A selective increase in particulate superoxide dismutase activity in parkinsonian substantia nigra. J Neurochem 53, 692-697.

Saitoh, M., Nishitoh, H., Fujii, M., Takeda, K., Tobiume, K., Sawada, Y., Kawabata, M., Miyazono, K., Ichijo, H., 1998. Mammalian thioredoxin is a direct inhibitor of apoptosis signal-regulating kinase (ASK) 1. The EMBO journal 17, 2596-2606.

Sanchez-Fernandez, R., Fricker, M., Corben, L.B., White, N.S., Sheard, N., Leaver, C.J., Van Montagu, M., Inze, D., May, M.J., 1997. Cell proliferation and hair tip growth in the Arabidopsis root are under mechanistically different forms of redox control. Proceedings of the National Academy of Sciences of the United States of America 94, 2745-2750.

Schenk, H., Klein, M., Erdbrugger, W., Droge, W., Schulze-Osthoff, K., 1994. Distinct effects of thioredoxin and antioxidants on the activation of transcription factors NF-kappa B and AP-1. Proceedings of the National Academy of Sciences of the United States of America 91, 1672-1676.

Seo, M.S., Kang, S.W., Kim, K., Baines, I.C., Lee, T.H., Rhee, S.G., 2000. Identification of a new type of mammalian peroxiredoxin that forms an intramolecular disulfide as a reaction intermediate. The Journal of biological chemistry 275, 20346-20354.

Shelton, M.D., Chock, P.B., Mieyal, J.J., 2005. Glutaredoxin: role in reversible protein s-glutathionylation and regulation of redox signal transduction and protein translocation. Antioxidants & redox signaling 7, 348-366.

Shenton, D., Grant, C.M., 2003. Protein S-thiolation targets glycolysis and protein synthesis in response to oxidative stress in the yeast Saccharomyces cerevisiae. The Biochemical journal 374, 513-519.

Shenton, D., Perrone, G., Quinn, K.A., Dawes, I.W., Grant, C.M., 2002. Regulation of protein S-thiolation by glutaredoxin 5 in the yeast Saccharomyces cerevisiae. The Journal of biological chemistry 277, 16853-16859.

Shi, J., Vlamis-Gardikas, A., Aslund, F., Holmgren, A., Rosen, B.P., 1999. Reactivity of glutaredoxins 1, 2, and 3 from Escherichia coli shows that glutaredoxin 2 is the primary hydrogen donor to ArsC-catalyzed arsenate reduction. The Journal of biological chemistry 274, 36039-36042.

Sian, J., Dexter, D.T., Lees, A.J., Daniel, S., Jenner, P., Marsden, C.D., 1994. Glutathione-related enzymes in brain in Parkinson's disease. Ann Neurol 36, 356-361.

Silva, G.M., Netto, L.E., Discola, K.F., Piassa-Filho, G.M., Pimenta, D.C., Barcena, J.A., Demasi, M., 2008. Role of glutaredoxin 2 and cytosolic thioredoxins in cysteinyl-based redox modification of the 20S proteasome. The FEBS journal 275, 2942-2955.

Sofic, E., Lange, K.W., Jellinger, K., Riederer, P., 1992. Reduced and oxidized glutathione in the substantia nigra of patients with Parkinson's disease. Neurosci Lett 142, 128-130.

Sofic, E., Riederer, P., Heinsen, H., Beckmann, H., Reynolds, G.P., Hebenstreit, G., Youdim, M.B., 1988. Increased iron (III) and total iron content in post mortem substantia nigra of parkinsonian brain. J Neural Transm 74, 199-205.

Srinivasan, U., Mieyal, P.A., Mieyal, J.J., 1997. pH profiles indicative of rate-limiting nucleophilic displacement in thioltransferase catalysis. Biochemistry 36, 3199-3206.

Stewart, E.J., Aslund, F., Beckwith, J., 1998. Disulfide bond formation in the Escherichia coli cytoplasm: an in vivo role reversal for the thioredoxins. The EMBO journal 17, 5543-5550.

Storr, S.J., Woolston, C.M., Zhang, Y., Martin, S.G., 2013. Redox environment, free radical, and oxidative DNA damage. Antioxidants & redox signaling 18, 2399-2408.

Terlecky, S.R., Terlecky, L.J., Giordano, C.R., 2012. Peroxisomes, oxidative stress, and inflammation. World J Biol Chem 3, 93-97.

Toledano, M.B., Kumar, C., Le Moan, N., Spector, D., Tacnet, F., 2007. The system biology of thiol redox system in Escherichia coli and yeast: differential functions in oxidative stress, iron metabolism and DNA synthesis. FEBS letters 581, 3598-3607.

Toyokuni, S., Okamoto, K., Yodoi, J., Hiai, H., 1995. Persistent oxidative stress in cancer. FEBS letters 358, 1-3.

Trotter, E.W., Grant, C.M., 2003. Non-reciprocal regulation of the redox state of the glutathione-glutaredoxin and thioredoxin systems. EMBO reports 4, 184-188.

Wang, J., Boja, E.S., Tan, W., Tekle, E., Fales, H.M., English, S., Mieyal, J.J., Chock, P.B., 2001. Reversible glutathionylation regulates actin polymerization in A431 cells. The Journal of biological chemistry 276, 47763-47766.

Watson, W.H., Pohl, J., Montfort, W.R., Stuchlik, O., Reed, M.S., Powis, G., Jones, D.P., 2003. Redox potential of human thioredoxin 1 and identification of a second dithiol/disulfide motif. The Journal of biological chemistry 278, 33408-33415.

Wells, W.W., Xu, D.P., Yang, Y.F., Rocque, P.A., 1990. Mammalian thioltransferase (glutaredoxin) and protein disulfide isomerase have dehydroascorbate reductase activity. The Journal of biological chemistry 265, 15361-15364.

Wood, Z.A., Poole, L.B., Hantgan, R.R., Karplus, P.A., 2002. Dimers to doughnuts: redox-sensitive oligomerization of 2-cysteine peroxiredoxins. Biochemistry 41, 5493-5504.

Wood, Z.A., Schroder, E., Robin Harris, J., Poole, L.B., 2003. Structure, mechanism and regulation of peroxiredoxins. Trends in biochemical sciences 28, 32-40.

Worthington, D.J., Rosemeyer, M.A., 1976. Glutathione reductase from human erythrocytes. Catalytic properties and aggregation. European journal of biochemistry / FEBS 67, 231-238.

Xiao, R., Lundstrom-Ljung, J., Holmgren, A., Gilbert, H.F., 2005. Catalysis of thiol/disulfide exchange. Glutaredoxin 1 and protein-disulfide isomerase use

different mechanisms to enhance oxidase and reductase activities. The Journal of biological chemistry 280, 21099-21106.

Yang, Y., Jao, S., Nanduri, S., Starke, D.W., Mieyal, J.J., Qin, J., 1998. Reactivity of the human thioltransferase (glutaredoxin) C7S, C25S, C78S, C82S mutant and NMR solution structure of its glutathionyl mixed disulfide intermediate reflect catalytic specificity. Biochemistry 37, 17145-17156.

Yang, Y.F., Wells, W.W., 1991. Catalytic mechanism of thioltransferase. The Journal of biological chemistry 266, 12766-12771.

Zaffagnini, M., Bedhomme, M., Lemaire, S.D., Trost, P., 2012. The emerging roles of protein glutathionylation in chloroplasts. Plant science : an international journal of experimental plant biology 185-186, 86-96.

Zaffagnini, M., Michelet, L., Marchand, C., Sparla, F., Decottignies, P., Le Marechal, P., Miginiac-Maslow, M., Noctor, G., Trost, P., Lemaire, S.D., 2007. The thioredoxin-independent isoform of chloroplastic glyceraldehyde-3-phosphate dehydrogenase is selectively regulated by glutathionylation. The FEBS journal 274, 212-226.

Zhao, J., Lu, Y., Shen, H.M., 2012. Targeting p53 as a therapeutic strategy in sensitizing TRAIL-induced apoptosis in cancer cells. Cancer letters 314, 8-23.

Zheng, M., Aslund, F., Storz, G., 1998. Activation of the OxyR transcription factor by reversible disulfide bond formation. Science 279, 1718-1721.

Zitka, O., Skalickova, S., Gumulec, J., Masarik, M., Adam, V., Hubalek, J., Trnkova, L., Kruseova, J., Eckschlager, T., Kizek, R., 2012. Redox status expressed as GSH:GSSG ratio as a marker for oxidative stress in paediatric tumour patients. Oncology letters 4, 1247-1253.

Appendix 1

PySCeS code listings

A1. Monothiol model

FIX: PSSG PSH NADPH NADP

R1: GSSG + NADPH = GSH + GSH + NADP

kcat1*GR*GSSG*NADPH/(Kgssg*Knadph)/((1+GSSG/Kgssg)*(1+NADPH/Knadph))

R2: GrxSSG + GSH = $Grx(SH)_2$ + GSSG

k2*GrxSSG*GSH*(1-(($Grx(SH)_2$*GSSG/GrxSSG*GSH)/Keq2))

R3: $Grx(SH)_2$ + PSSG = GrxSSG + PSH

k3*$Grx(SH)_2$*PSSG

A2. Dithiol model

FIX: PSSG PSH NADPH NADP GSHp

R1: GSSG + NADPH = {2} GSH + NADP

kcat1*GR*GSSG*NADPH/(Kgssg*Knadph)/((1+GSSG/Kgssg)*(1+NADPH/Knadph))

R2: GrxSS + {2} GSH = $Grx(SH)_2$ + GSSG

k2*((GrxSS*(GSH**2)) - ($Grx(SH)_2$*GSSG)/Keq2)

R3: $Grx(SH)_2$ + PSSG = GrxSS + PSH + GSHp

k3*$Grx(SH)_2$*PSSG

Appendix 2

Table A1. Parameters and values for fitting *Escherichia coli* Grx1 substrate saturation datasets of Peltoniemi *et al.* 2006

	Value	Reference
Metabolite	**(µM)**	
NADPH	50	Peltoniemi *et al.*, 2006
NADP	1	-
GSH	998	Peltoniemi *et al.*, 2006
GSSG	1	Peltoniemi *et al.*, 2006
PSSG	1	Peltoniemi *et al.*, 2006
PSH	1	-
Redoxin	**(µM)**	
$Grx(SH)_2$	0.01	Peltoniemi *et al.*, 2006
GrxSS	0.01	Peltoniemi *et al.*, 2006
Glutathione reductase		
K_{NADPH}	3.8 µM	Williams, 1976
K_{GSSG}	55 µM	Williams, 1976
k_{cat}	500 s^{-1}	Massey and Williams, 1965
[Glutathione reductase]	0.02 µM	Peltoniemi *et al.*, 2006

Table A2. Parameters and values for fitting yeast Grx1 and Grx2 HEDS datasets of Li *et al.* 2010

	Value		Reference
	Grx1	**Grx2**	
Metabolite	**(µM)**	**(µM)**	
NADPH	250	250	Li *et al.*, 2010
NADP	1	1	-
GSH	998	998	Li *et al*., 2010
GSSG	1	1	Li *et al*., 2010
PSSG	70	70	Li *et al*., 2010
PSH	1	1	-
Redoxin	**(µM)**	**(µM)**	
$Grx(SH)_2$	0.12	0.02	Li *et al*., 2010
GrxSS	0.12	0.02	Li *et al*., 2010
Glutathione reductase			
K_{NADPH}	15 µM	15 µM	Yu and Zhou, 2007
K_{GSSG}	74.6 µM	74.6 µM	Yu and Zhou, 2007
k_{cat}	900 s^{-1}	900 s^{-1}	Yu and Zhou, 2007
[Glutathione reductase]	0.02 µM	0.02 µM	Li *et al*., 2010

Table A3. Parameters and values for fitting yeast Grx1 glutathione datasets of Discola *et al*. 2009

	Value	Reference
Metabolite	**(µM)**	
NADPH	200	Discola *et al.*, 2009
NADP	1	-
GSH	998	Discola *et al.*, 2009
GSSG	1	
PSSG	30	Discola *et al.*, 2009
PSH	1	-
Redoxin	**(µM)**	
$Grx(SH)_2$	0.25	Discola *et al.*, 2009
GrxSS	0.25	Discola *et al.*, 2009
Glutathione reductase		
K_{NADPH}	15 µM	Yu and Zhou, 2007
K_{GSSG}	74.6 µM	Yu and Zhou, 2007
k_{cat}	900 s^{-1}	Yu and Zhou, 2007
[Glutathione reductase]	0.02 µM	Discola *et al.*, 2009

Appendix 3

Python Scripts

1. Time course simulations

```
import os
backupdir = os.getcwd()

import numpy
import scipy
import pylab
import pysces
import time
pysces.PyscesModel.model_dir=backupdir
pysces.PyscesModel.output_dir=backupdir
os.chdir(backupdir)
from pylab import *

# get data
m=pysces.model('dithiol_core')
m.doStateShow()
m.SetQuiet()
m.showConserved()
m.showODE()
m.doSim(end = 250, points = 100)
f, c = m.data_sim.getSpecies(lbls=True)
b = []
for i in range(len(c)-1):
    b.append((c[i+1], i+1))

print '\nScan labels:\n'
for i in range(len(b)):
    print b[i]
```

```
pylab.rc('font', family = 'sans-serif')
pylab.rc('xtick', labelsize = 10)
pylab.rc('ytick', labelsize = 10)
pylab.rc('ytick.major', pad = 8)
pylab.rc('ytick.minor', pad = 8)
pylab.rc('axes', labelsize = 12)
pylab.rc('legend', fontsize = 12)
pylab.rc('legend', axespad = 0.02)
pylab.rc('legend', handletextsep = 0.09)

ioff()
fig=pylab.figure()
ax = fig.add_subplot(222)
ax.plot(f[:,0], f[:,1], 'r--', label='GSSG' )
ax.plot(f[:,0], f[:,2], 'b-', label='GSH' )
ax.plot(f[:,0], f[:,3], 'b-', label='GrxSSGSH' )
ax.plot(f[:,0], f[:,4], 'r--', label='GrxSH2' )
plt.ylabel(r'[Species] ($\mu$M)')
plt.xlabel(r'Time (s)')
pylab.draw()

def save_fig(name='simulations.png'):
    pylab.draw()
    pylab.savefig(name)

if __name__ == "__main__":
    draw()
    show()
    time.sleep(15)
    pylab.close()
    os.chdir(backupdir)
```

2. Kinetic behaviour of the realistic dithiol model

```
import os
backupdir = os.getcwd()
import numpy
import scipy
import pylab
import pysces
import time
pysces.PyscesModel.MODEL_DIR=backupdir
pysces.PyscesModel.OUTPUT_DIR=backupdir
os.chdir(backupdir)
from pylab import *

m=pysces.model('dithiol_core')
m.doLoad()
m.doStateShow()
m.SetQuiet()
#m.GSSG_init=0
#m.GSH_init=1
m.scan_in= 'PSSG'
m.scan_out= ['J_R1']
scan_range=scipy.logspace(-3, 3, 101)
m.Scan1(scan_range)
f=m.scan_res
o=1/f

# configure text stuff
pylab.rc('font', family = 'sans-serif')
pylab.rc('xtick', labelsize = 10)
pylab.rc('ytick', labelsize = 10)
pylab.rc('ytick.major', pad = 8)
pylab.rc('ytick.minor', pad = 8)
pylab.rc('axes', labelsize = 12)
```

```
pylab.rc('legend',  fontsize  = 12)
#pylab.rc('legend',  axespad = 0.02)
#pylab.rc('legend',  handletextsep  = 0.05)

# create da figure
ioff()
fig=pylab.figure()
ax = fig.add_subplot(222)
plt.ylabel(r'1/v  (s.$\mu$M$^{-1}$)')
plt.xlabel(r'1/PSSG  ($\mu$M)$^{-1}$')
ax.plot(o[:,0],  o[:,1],  'k-', label='model'  )
pylab.draw()

def setFigLabels(x='X-axis',  y='Y-axis'):
    ax.set_xlabel(x)
    ax.set_ylabel(y)

def save_fig(name='PSSG_recip.png'):
    pylab.draw()
    pylab.savefig(name)

if __name__  == "__main__":
    draw()
    show()
    save_fig()
    time.sleep(15)
    pylab.close()
    os.chdir(backupdir)
```

3. Reciprocal kinetic plots

```
import os
backupdir = os.getcwd()
import numpy
import scipy
import pylab
import pysces
import time
pysces.PyscesModel.MODEL_DIR=backupdir
pysces.PyscesModel.OUTPUT_DIR=backupdir
os.chdir(backupdir)
from pylab import *

m=pysces.model('dithiol_core_rev')
m.doLoad()
m.doStateShow()
m.SetQuiet()

m.GSH_init = 0.25
m.GSSG_init = 0
m.scan_in= 'PSSG'
m.scan_out= ['J_R1']
scan_range=scipy.logspace(-1, 0.01, 100)
m.Scan1(scan_range)
h=m.scan_res
#f=1/h

m.GSH_init = 0.3
m.GSSG_init = 0
m.scan_in= 'PSSG'
m.scan_out= ['J_R1']
m.Scan1(scan_range)
i=m.scan_res
```

```
#j=1/i

m.GSH_init  = 0.4
m.GSSG_init  = 0
m.scan_in=  'PSSG'
m.scan_out=  ['J_R1']
m.Scan1(scan_range)
k=m.scan_res
#l=1/k

m.GSH_init  = 0.6
m.GSSG_init  = 0
m.scan_in=  'PSSG'
m.scan_out=  ['J_R1']
m.Scan1(scan_range)
n=m.scan_res
#o=1/n

o=pysces.model('dithiol_core')
o.doLoad()
o.doStateShow()
o.SetQuiet()
o.Keq2 = 100
o.GSH_init  = 0.25
o.GSSG_init  = 0
o.scan_in=  'PSSG'
o.scan_out=  ['J_R1']
scan_range=scipy.logspace  (-1, 0.01, 100)
o.Scan1(scan_range)
x=o.scan_res
#f=1/h
```

```
o.GSH_init  = 0.3
o.GSSG_init  = 0
o.scan_in=  'PSSG'
o.scan_out=  ['J_R1']
o.Scan1(scan_range)
y=o.scan_res
#j=1/i

o.GSH_init  = 0.4
o.GSSG_init  = 0
o.scan_in=  'PSSG'
o.scan_out=  ['J_R1']
o.Scan1(scan_range)
w=o.scan_res
#l=1/k

o.GSH_init  = 0.6
o.GSSG_init  = 0
o.scan_in=  'PSSG'
o.scan_out=  ['J_R1']
o.Scan1(scan_range)
v=o.scan_res
#o=1/n

#~ # configure  text stuff
pylab.rc('font',  family  = 'sans-serif')
pylab.rc('xtick',  labelsize  = 10)
pylab.rc('ytick',  labelsize  = 10)
pylab.rc('ytick.major',  pad = 8)
pylab.rc('ytick.minor',  pad = 8)
pylab.rc('axes',  labelsize  = 12)
pylab.rc('legend',  fontsize  = 12)
#pylab.rc('legend',  axespad = 0.02)
#pylab.rc('legend',  handletextsep  = 0.09)
```

```
# create da figure
ioff()
fig=pylab.figure()
ax = fig.add_subplot(221)

ax.plot(h[:,0],  h[:,1],  'k-', label='GSH=2'  )
ax.plot(i[:,0],  i[:,1],  'b-', label='GSH=3'  )
ax.plot(k[:,0],  k[:,1],  'r-', label='GSH=4'  )
ax.plot(n[:,0],  n[:,1],  'g-', label='GSH=5'  )
ax.plot(x[:,0],  x[:,1],  'k--', label='GSH=2' )
ax.plot(y[:,0],  y[:,1],  'b--', label='GSH=3' )
ax.plot(w[:,0],  w[:,1],  'r--', label='GSH=4' )
ax.plot(v[:,0],  v[:,1],  'g--', label='GSH=5' )
#ax.legend(loc=4)
#plt.xmin  = 10
plt.ylabel(r'v  ($\mu$M$s^{-1})$')
plt.xlabel(r'PSSG($\mu$M)')

ax = fig.add_subplot(222)
ax.plot(h[:,0],  h[:,1],  'k-', label='GSH=2'  )
ax.plot(i[:,0],  i[:,1],  'b-', label='GSH=3'  )
ax.plot(k[:,0],  k[:,1],  'r-', label='GSH=4'  )
ax.plot(n[:,0],  n[:,1],  'g-', label='GSH=5'  )
#ax.legend(loc=4)
#plt.xmin  = 10
plt.ylabel(r'v  ($\mu$M$s^{-1})$') #(s.$\mu$M$^{-1})$
plt.xlabel(r'PSSG($\mu$M)')


ax = fig.add_subplot(223)
ax.plot(x[:,0],  x[:,1],  'k--', label='GSH=2' )
ax.plot(y[:,0],  y[:,1],  'b--', label='GSH=3' )
ax.plot(w[:,0],  w[:,1],  'r--', label='GSH=4' )
```

```
ax.plot(v[:,0],  v[:,1],  'g--', label='GSH=5'  )
#ax.legend(loc=4)
#plt.xmin  = 10
plt.ylabel(r'v  ($\mu$M$s^{-1})$')
plt.xlabel(r'PSSG($\mu$M)')
pylab.draw()

fig.subplots_adjust(hspace=0.4)
fig.subplots_adjust(wspace=0.4)

def save_fig(name='pssg_rev_irr_.png'):
    pylab.draw()
    pylab.savefig(name)

if __name__ == "__main__":
    draw()
    show()
    save_fig()
    time.sleep(15)
    pylab.close()
    os.chdir(backupdir)
```

4. Nonlinear least squares analysis of Discola (Grx1) data

```
import os
backupdir = os.getcwd()
import numpy
import scipy
import pylab
import pysces
import time
pysces.PyscesModel.MODEL_dir=backupdir
pysces.PyscesModel.OUTPUT_dir=backupdir
os.chdir(backupdir)
from pylab import *

# get data
f1a = numpy.loadtxt('peltp.csv')    # Grx (tot), J_R1

# instantiate model
m=pysces.model('pelt_model',backupdir)
m.doLoad()
m.doStateShow()
m.SetQuiet()
m.scan_in='PSSG'
m.scan_out=['J_R1']
scan_range=scipy.logspace (-1, 4, 501)
m.Scan1(scan_range)
f=m.scan_res

# configure text stuff
pylab.rc('font', family = 'sans-serif')
pylab.rc('xtick', labelsize = 8)
pylab.rc('ytick', labelsize = 10)
pylab.rc('ytick.major', pad = 8)
```

```
pylab.rc('ytick.minor',  pad = 8)
pylab.rc('axes',  labelsize  = 12)
pylab.rc('legend',  fontsize  = 12)
#pylab.rc('legend',  axespad = 0.02)
#pylab.rc('legend',  handletextsep  = 0.05)
##  pylab.rc('legend',  labelsep  = 0.02)
##  pylab.rc('legend',  pad = 0.3)

# generate  model  data  for  fit  conditions
def genmodeldata(m,  p, scanpar,  xrange):
    k2, k3 = p
    m.k2 = k2
    m.k3 = k3
    m.scan_in  = scanpar
    m.scan_out  = ['J_R1']
    m.Scan1(xrange)
    return  m.scan_res

def residuals(p,  expdata):
    modeldata  = genmodeldata(m,  p, 'PSSG', expdata[:,0])[:,1]
    err = expdata[:,1]  - modeldata
    return  err

def fitexp(expdata,  p0, plot=0):
    df = len(expdata)-len(p0)
    ydata  = expdata[:,1]
    xdata  = expdata[:,0]
    SStot = sum((ydata-scipy.mean(ydata))**2)
    plsq  = scipy.optimize.leastsq(residuals,  p0, args=(expdata),  full_output=1)
    pfit  = plsq[0]
    cov_x = plsq[1]
    fin_residuals  = plsq[2]['fvec']
    SSQ = sum((fin_residuals)**2)
    SE = scipy.sqrt(SSQ/df*scipy.diag(cov_x))
```

```
    SD = scipy.sqrt(SSQ/len(fin_residuals))
    Rsq = 1.0-SSQ/SStot
    if plot:
        mdata = genmodeldata(m, pfit, 'PSSG', scipy.linspace(xdata[0], xdata[-1], 100))
        plotdata(expdata, mdata)
        print 'Rsq', Rsq
    return {'pfit':pfit, 'SE':SE, 'SSQ':SSQ, 'SD':SD, 'Rsq':Rsq, 'df':df, 'cov_x':cov_x, 'plsq':plsq}

ioff()
fig=pylab.figure()
ax = fig.add_subplot(222)
plt.ylabel(r'$v$ ($\mu$M s$^{-1}$)')
plt.xlabel(r'PSSG ($\mu$M)$')
pylab.draw()

def plotdata(expdata, modeldata):
        ax.plot(expdata[:,0], expdata[:,1], 'ko',label='data')
        ax.plot(modeldata[:,0], modeldata[:,1], 'k-',label='model')
        pylab.draw()

def save_fig(name='Pelt_ePSSG.png'):
    pylab.draw()
    pylab.savefig(name)

if __name__ == "__main__":
    data1 = f1a
    p0 = scipy.copy((m.k2, m.k3))
    fit1 = fitexp(data1, p0, plot=1)
    print 'fitted values:'
    print 'k2:   ', fit1['pfit'][0], ' +- ', fit1['SE'][0]
    print 'k3:   ', fit1['pfit'][1], ' +- ', fit1['SE'][1]
    save_fig()
    pylab.close()
    os.chdir(backupdir)
```